Cairo University

Faculty of Engineering

Electronics & Communication Department

ELC3050 Project

Design and Analysis of a 2-Element Probe-Fed Microstrip Patch Antenna Operating at 20 GHz

Under supervision of Dr Islam Eshra

Name	ID
يوسف خالد عمر محمود	9220984
مصطفى أحمد حسني محمود درويش	9220832
مصطفى فتحي محمد حسن عسكر	9220844
يوسف اشرف محمد	9220972
عمر احمد رجب	9220513
عمر ايمن امين	9220528

Table of Contents

Table of Figures

1. Introduction and Problem Definition

Abstract

This report dives into the design and analysis of a 2-element probe-fed microstrip patch antenna operating at 20 GHz, catering to high-frequency communication systems such as satellite communication, millimeter-wave networks, and radar systems. The project aims to achieve optimal performance characterized by high gain, low return loss (S11 < -10 dB), and enhanced radiation efficiency. By incorporating innovative design strategies, including impedance matching networks and bandwidth enhancement techniques, the study explores the trade-offs and optimizations required for an efficient antenna system.

Electromagnetic (EM) simulation tools are utilized to optimize critical parameters such as gain, bandwidth, and radiation pattern while analyzing mutual coupling and element spacing effects. The final design is validated through simulation results, ensuring compliance with the stringent requirements of modern high-frequency applications.

Introduction

With the increasing demand for efficient and compact communication systems, the design of antennas operating at millimeter-wave frequencies has become crucial. The 20 GHz band is of particular interest due to its application in satellite communication, radar systems, and emerging 5G technologies. Microstrip patch antennas, with their low profile, ease of fabrication, and compatibility with planar and non-planar surfaces, have emerged as a preferred choice for these applications.

The primary challenge in designing microstrip patch antennas lies in their inherently narrow bandwidth, which limits their utility in wideband applications. Probe-fed microstrip antennas are particularly prone to this limitation, necessitating the implementation of techniques to enhance bandwidth without compromising other performance metrics like gain and efficiency. Additionally, designing antenna arrays introduces complexities such as mutual coupling and beam pattern distortion, which must be mitigated to achieve the desired performance.

This project focuses on the design and analysis of a 2-element probe-fed microstrip patch antenna array optimized for operation at 20 GHz. Key design objectives include achieving an S11 below -10 dB, maximizing gain and radiation efficiency, and addressing mutual coupling and element spacing to enhance array performance. The project employs EM simulation tools to validate the design and optimize its parameters, providing insights into the trade-offs involved in high-frequency antenna design.

Problem Statement

To design a 2-element array of probe-fed microstrip patch antennas operating at 20 GHz, achieving optimal performance in terms of bandwidth, gain, and radiation efficiency, while addressing mutual coupling and beam pattern alignment.

Significance of Microstrip Patch Antennas

Microstrip patch antennas are integral to modern high-frequency communication systems due to their compact size, lightweight, and ease of integration with other RF components. At 20 GHz, these antennas are particularly advantageous for:

- **Satellite Communication:** Providing robust and directional communication links.
- **Radar Systems:** Offering precise detection and ranging capabilities.
- **5G Networks:** Addressing the high bandwidth and directional requirements of next-generation wireless communication.

The probe-fed configuration is widely used for its simplicity and compatibility with various substrates but requires careful impedance matching and design optimizations to achieve the desired performance metrics.

Challenges in Design

Designing probe-fed microstrip patch antennas at 20 GHz presents several challenges:

1. **Narrow Bandwidth:**
    - Achieving a wider bandwidth is critical for accommodating high data rates and minimizing signal distortion. Techniques such as impedance matching networks, substrate thickness adjustments, and the use of stacked patches are explored.
2. **Mutual Coupling:**
    - In an array configuration, the interaction between elements can degrade radiation patterns and efficiency. Optimal element spacing and the use of decoupling structures are crucial to mitigate these effects.
3. **Gain and Directivity:**
    - High gain and precise directivity are essential for extending communication range and focusing the radiated energy. The use of optimized feed networks and element configurations ensures these attributes.
4. **Impedance Matching:**
    - Proper impedance matching is necessary to minimize reflection losses and ensure maximum power transfer. The design incorporates impedance tuning at the feed point to achieve this.
5. **Radiation Pattern Stability:**
    - Ensuring symmetrical and stable radiation patterns across the operating frequency band is crucial for reliable performance. This requires addressing feed network asymmetries and optimizing element alignment.

Performance Metrics

The design aims to optimize the following key performance metrics:

- **Return Loss (S11):** Below -10 dB at the operating frequency.
- **Bandwidth:** Enhanced to accommodate high-frequency applications.
- **Gain:** Maximized for directional communication.
- **Radiation Efficiency:** High efficiency to minimize power losses.
- **Mutual Coupling:** Minimized to improve array performance.
- **Impedance Matching:** Ensuring optimal input impedance for efficient power transfer.

By addressing these challenges, the project seeks to develop a robust and efficient 2-element microstrip patch antenna array tailored for modern communication needs.

project involves the design of a 2-element probe-fed microstrip patch antenna operating at 20 GHz. The goal is to achieve an S11 less than -10 dB at the operating frequency while optimizing performance in terms of bandwidth, gain, and radiation efficiency. A comprehensive analysis of the antenna's mutual coupling and gain vs. element spacing is also included.

Verification Against Another Source

We're going to simulate a dipole with the design in figure 9.9 in refrence [1] with HFSS.

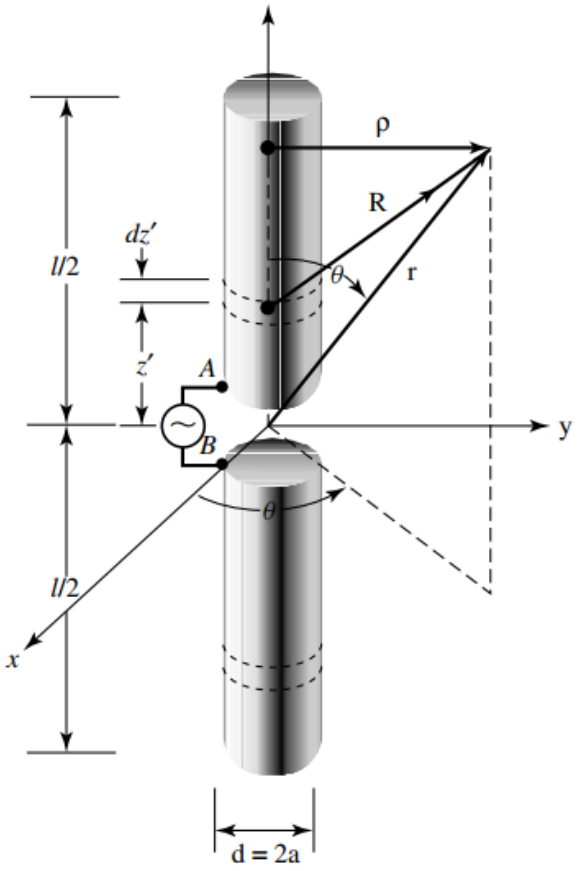

Figure 9.9 Center-fed cylindrical antenna configuration.

With values that's applied in Table 1:

Name	Unit	"Evaluated Value"	Description
dl	mm	139.5mm	Antenna length
rdi	mm	0.2625mm	Antenna radius
gap_L	mm	1mm	Gap length

Table 1:Diploe Antenna Dimensions

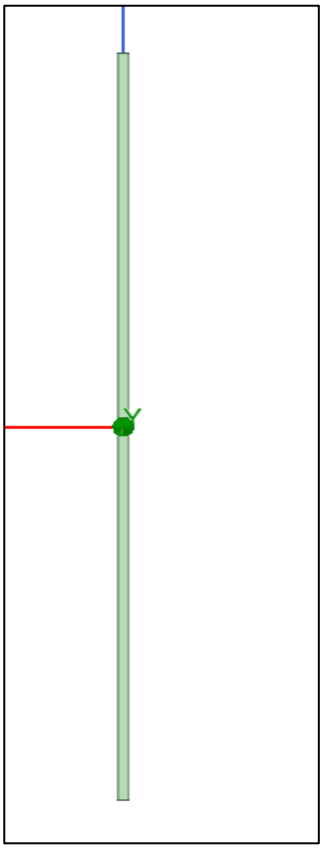

Figure 1: dipole antenna designed for verification

Benchmark Description

- A dipole antenna is a standard reference in antenna theory, with well-documented characteristics such as impedance, radiation pattern, and gain.
- It is widely used as a baseline for verifying simulation accuracy and comparing performance metrics.

Simulation Setup

1. **Design Parameters**:
    - Length of the dipole: L=$\boldsymbol{\lambda/2}$ $\boldsymbol{\lambda}$ is the wavelength at the operating frequency.
    - Material: Mention the conductor used (copper or PEC).

2. **Simulation Environment**:
    - Define the simulation parameters, such as mesh size, boundary conditions, and excitation type (e.g., lumped port or wave port).
3. **Performance Metrics Evaluated**:
    - Return Loss (S11).
    - Radiation patterns in E-plane and H-plane.
    - Gain and efficiency.

Equations Controlling Dipole Antenna

1. **Directivity**:

$$\boldsymbol{D = 1.64}\ (\boldsymbol{2.15\ dBi\ for\ a\ half - wavelength\ dipole}).$$

2. **Radiation Pattern**:
    - E-plane pattern: $\boldsymbol{E(\theta) = E0sin(\theta)}$ for $\boldsymbol{0 \leq \theta \leq \pi}$.
    - H-plane pattern: $\boldsymbol{E(\phi) = constant}$ for $\boldsymbol{0 \leq \phi \leq 2\pi}$.
3. **Input Impedance**:

$$\boldsymbol{Zin = Rr + jX, where\ X\ is\ the\ reactance}.$$

4. **Gain**:

$$\boldsymbol{G = D \times \eta}$$

where $\boldsymbol{\eta}$ is the efficiency of the antenna.

Results Comparison

We are going to use Table 9.1 in refrence [1] to verfy. According to it I'm expecting Rin=67Ω

TABLE 9.1 Cylindrical Dipole Resonances

	First Resonance	Second Resonance	Third Resonance	Fourth Resonance
LENGTH	$0.48\lambda F$	$0.96\lambda F$	$1.44\lambda F$	$1.92\lambda F$
RESISTANCE (ohms)	67	$\frac{R_n^2}{67}$	95	$\frac{R_n^2}{95}$

$$F = \frac{l/2a}{1 + l/2a}; R_n = 150 \log_{10}(l/2a)$$

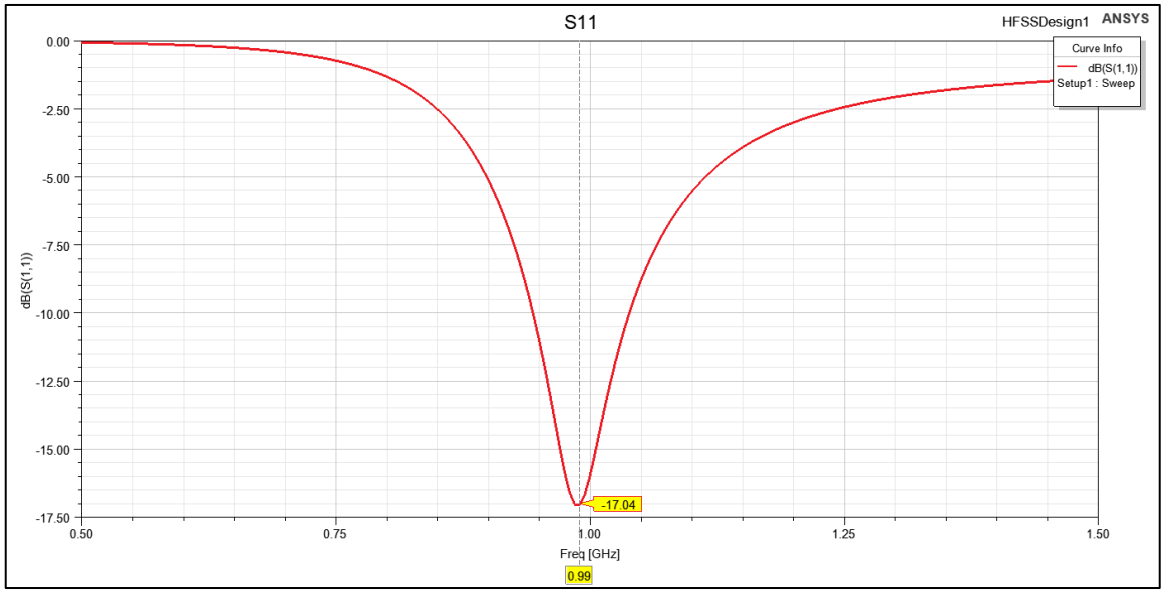

Figure 2: S11 for dipole antenna for verification

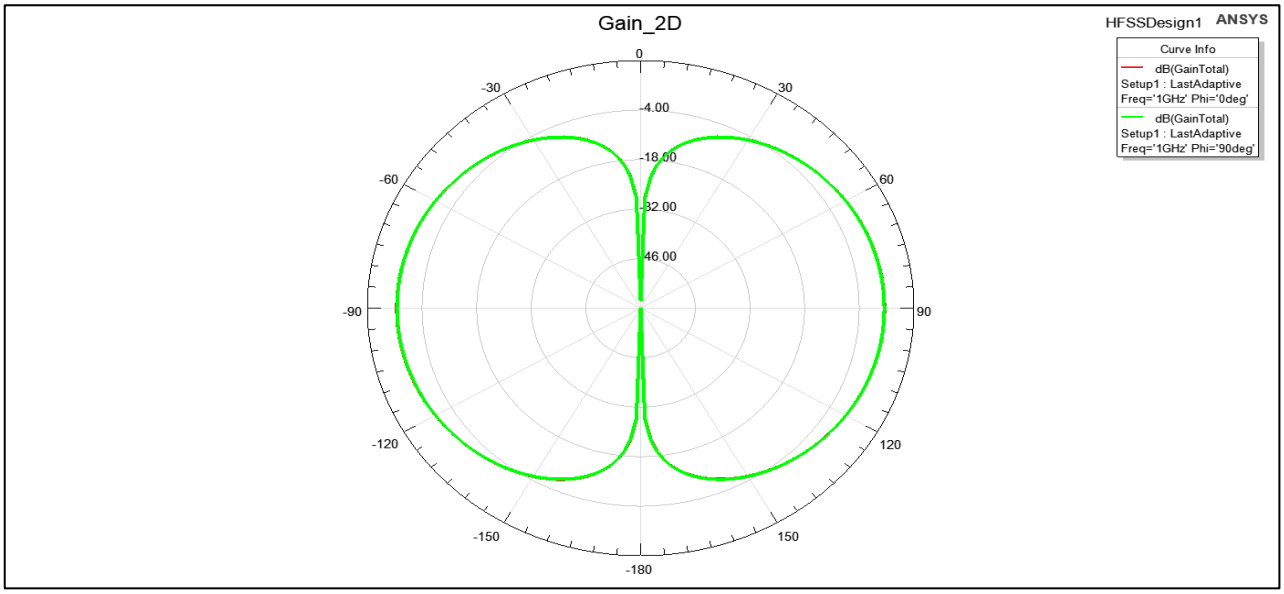

Figure 4: Gain 2D for dipole antenna for verification

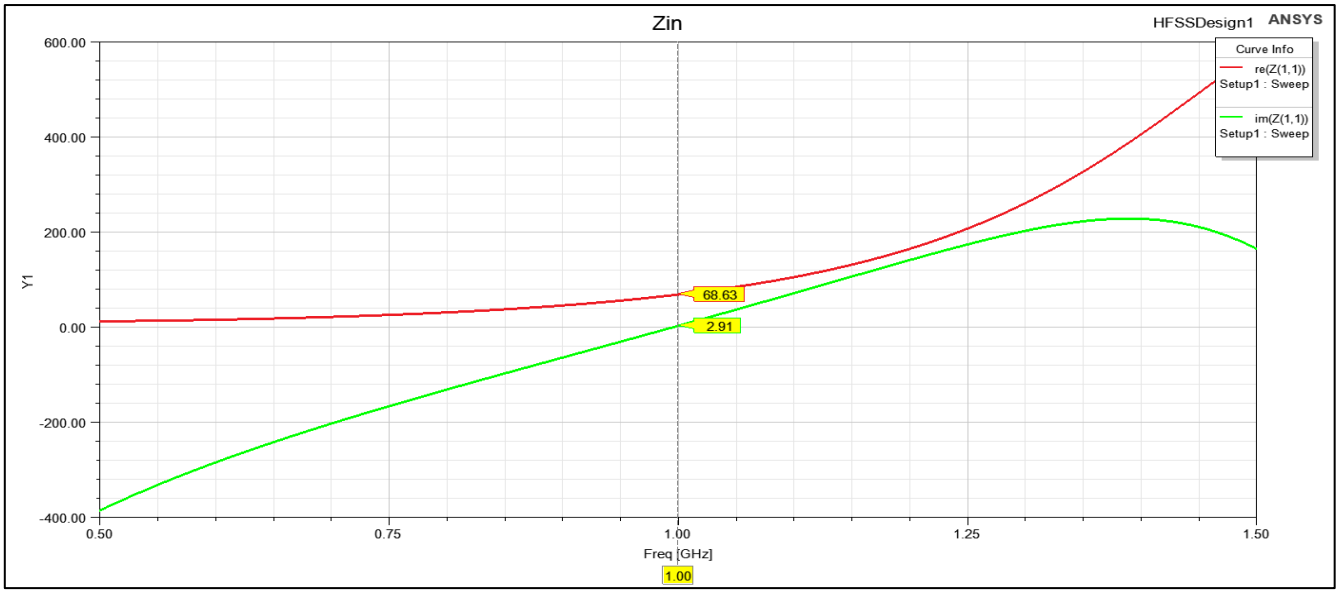

Figure 3: Zin for dipole antenna for verification

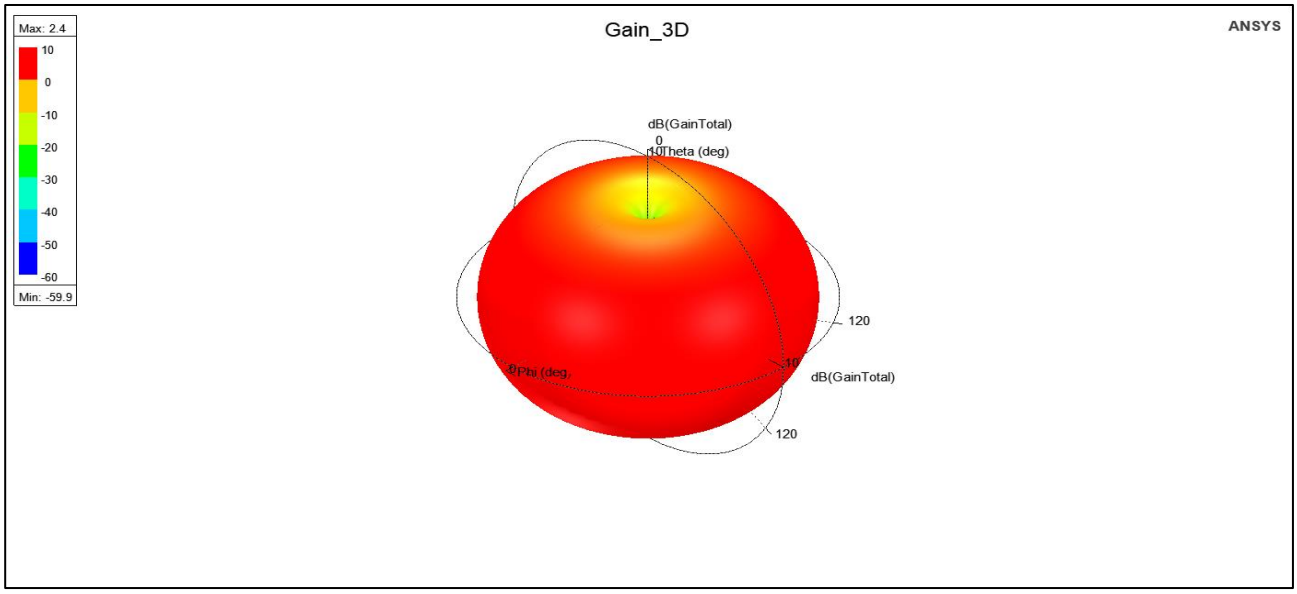

Figure 5: Gain 3D for dipole antenna for verification

Conclusion

- The dipole antenna serves as a reliable reference for verifying the EM simulation tool.
- imulated results of the dipole antenna matches theoretical expectations (S11 plot, radiation pattern, and gain).
- The Rin is 68.63 which is approximately equal to the theotical value in Table 9.1.

So the EM tool HFSS is verified

2. Design Procedure

The design started with the selection of the substrate material R04003C with a dielectric constant of 3.55. Initial dimensions were calculated using standard formulas for microstrip patch antennas, considering a substrate thickness of 0.406 mm. An online calculator was used to determine the initial patch dimensions, which were fine-tuned through simulation sweeps for optimal S11 performance.

A single patch antenna was first designed and analyzed to establish baseline performance metrics. Subsequently, a 2-element array was constructed with varying patch separation distances (dp) to study mutual coupling. A matching network was designed for probe feeding to further optimize the design.

At first, we started with the following mathematical modelling for our design then we tuned and swept parameters to achieve required specs.

Patch:

The resonant frequency of a rectangular microstrip patch antenna can be calculated using:[5]

$$f_r = \frac{c}{2L_{eff}\sqrt{\varepsilon_{eff}}}$$

where:

- c: Speed of light in free space ($3 \times 10^8 \text{m/s}$)
- L_{eff}: Effective length of the patch
- ε_{eff}: Effective dielectric constant of the substrate.

Effective Length:

- $L_{eff} = L + 2\Delta L$
  where:
- $\Delta L = 0.412.h \frac{(\varepsilon_{eff}+0.3)(w/h+0.264)}{(\varepsilon_{eff}-0.258)(w/h+0.8)}$

Substrate:

Effective dielectric constant:

$$\varepsilon_{eff} = \frac{\varepsilon_r + 1}{2} + \frac{\varepsilon_r - 1}{2}\left(1 + 12\frac{h}{W}\right)^{-1/2}$$

where:

- ε_r: Relative permittivity of the substrate

  We used RO4003C in Table 2 dielectric with $\varepsilon_r = 3.55$[4]

- h: Height of the substrate
- W: Width of the patch.

Property	Typical Value RO4003C	Typical Value RO4350B	Direction	Units	Condition	Test Method
Dielectric Constant, ε_r Process	3.38 ± 0.05	(1) 3.48 ± 0.05	Z	--	10 GHz/23°C	IPC-TM-650 2.5.5.5 Clamped Stripline
(2) Dielectric Constant, ε_r Design	3.55	3.66	Z	--	8 to 40 GHz	Differential Phase Length Method
Dissipation Factor tan, δ	0.0027 0.0021	0.0037 0.0031	Z	--	10 GHz/23°C 2.5 GHz/23°C	IPC-TM-650 2.5.5.5
Thermal Coefficient of ε_r	+40	+50	Z	ppm/°C	-50°C to 150°C	IPC-TM-650 2.5.5.5
Volume Resistivity	1.7 X 10^{10}	1.2 X 10^{10}		MΩ•cm	COND A	IPC-TM-650 2.5.17.1
Surface Resistivity	4.2 X 10^{9}	5.7 X 10^{9}		MΩ	COND A	IPC-TM-650 2.5.17.1
Electrical Strength	31.2 (780)	31.2 (780)	Z	KV/mm (V/mil)	0.51mm (0.020")	IPC-TM-650 2.5.6.2
Tensile Modulus	19,650 (2,850) 19,450 (2,821)	16,767 (2,432) 14,153, (2,053)	X Y	MPa (ksi)	RT	ASTM D638
Tensile Strength	139 (20.2) 100 (14.5)	203 (29.5) 130 (18.9)	X Y	MPa (ksi)	RT	ASTM D638
Flexural Strength	276 (40)	255 (37)		MPa (kpsi)		IPC-TM-650 2.4.4
Dimensional Stability	<0.3	<0.5	X,Y	mm/m (mils/inch)	after etch +E2/150°C	IPC-TM-650 2.4.39A
Coefficient of Thermal Expansion	11 14 46	10 12 32	X Y Z	ppm/°C	-55 to 288°C	IPC-TM-650 2.4.41
Tg	>280	>280		°C TMA	A	IPC-TM-650 2.4.24.3
Td	425	390		°C TGA		ASTM D3850
Thermal Conductivity	0.71	0.69		W/m/°K	80°C	ASTM C518
Moisture Absorption	0.06	0.06		%	48 hrs immersion 0.060" sample Temperature 50°C	ASTM D570

Table 2 RT-duroid 5870 - 5880 Data Sheet

2. Bandwidth Enhancement Analysis

Bandwidth (BW) is related to the quality factor (Q) by:

$$BW = \frac{f_r}{Q}$$

Technique used to improve bandwidth:

- **Impedance Matching**: Adding a matching network to reduce reflections.
    - Use Zin and Z0 to compute matching network:
    - $\Gamma = \frac{Zin-Z0}{Zin+Z0}$

3. Input Impedance

The input impedance at the feed point is given by:

$$Zin = Rin + jXin$$

where Rin and Xin are resistance and reactance components derived from field distributions.

4. Radiation Pattern

The far-field electric field components can be approximated as:

$$E_\theta = \frac{j\eta I0}{2\pi r}\sin\theta\cos(\frac{kL}{2}\sin\theta)$$

$$E_\phi = 0$$

where:

- $k = \frac{2\pi}{\lambda}$: Wave number
- r: Distance to observation point
- η: Intrinsic impedance of the medium.

5. Gain and Efficiency

Gain (G) and radiation efficiency (η_r) are related:

$$G = \eta_r \cdot D$$

where D is the directivity.

Efficiency:

$$\eta_r = \frac{Prad}{Pinput}$$

EM calculator:

We Initialized our design using Pasternack's **Microstrip Patch Antenna Calculator**[2]

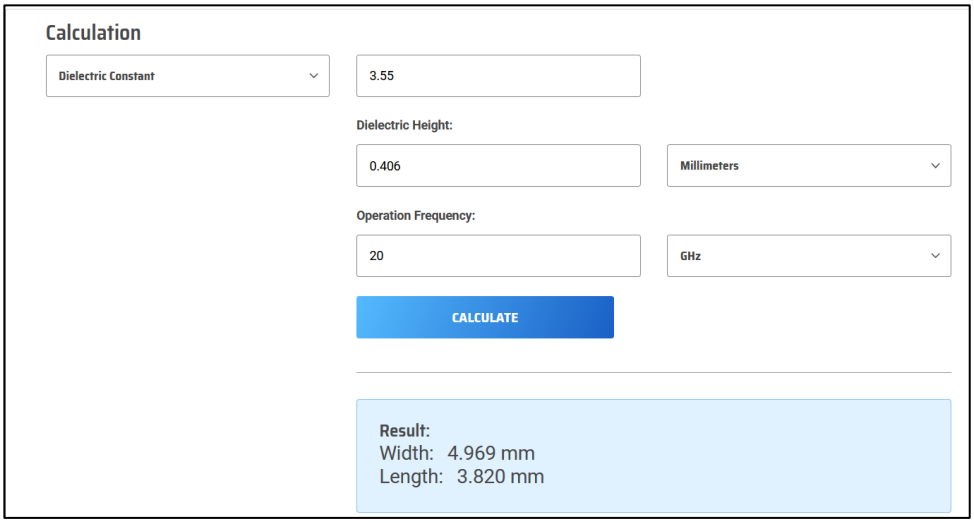

Figure 6 EM calculator results

In figure 6, we can see that we started with W = 4.969 mm and L = 3.82 mm then we swept them to get the specs in figure 7.

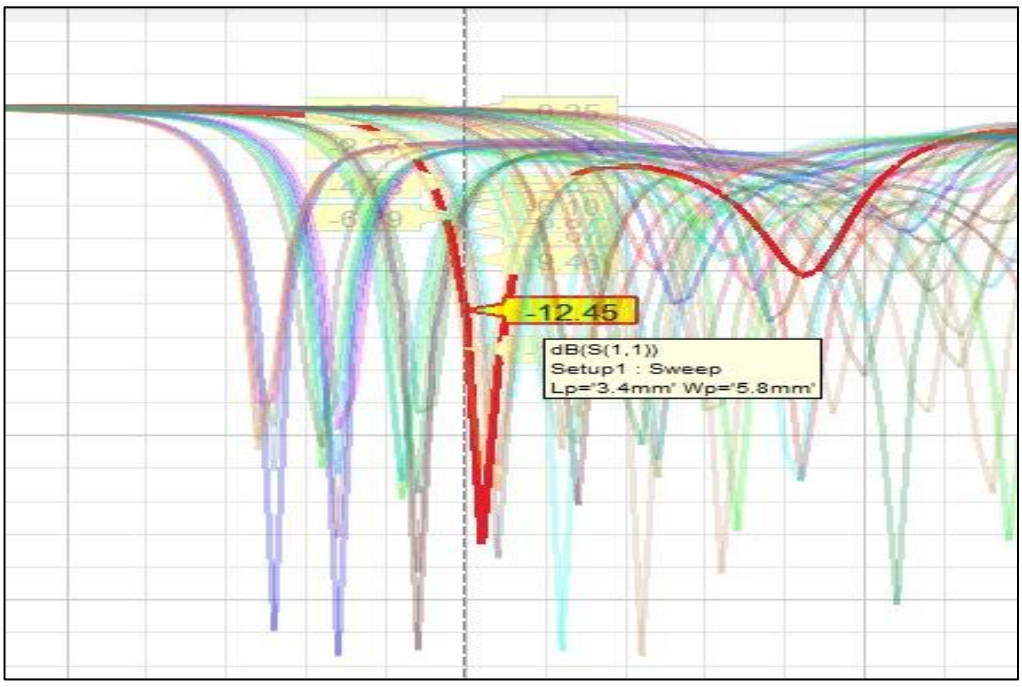

Figure 7 L,W S11 sweaping

Design of single patch

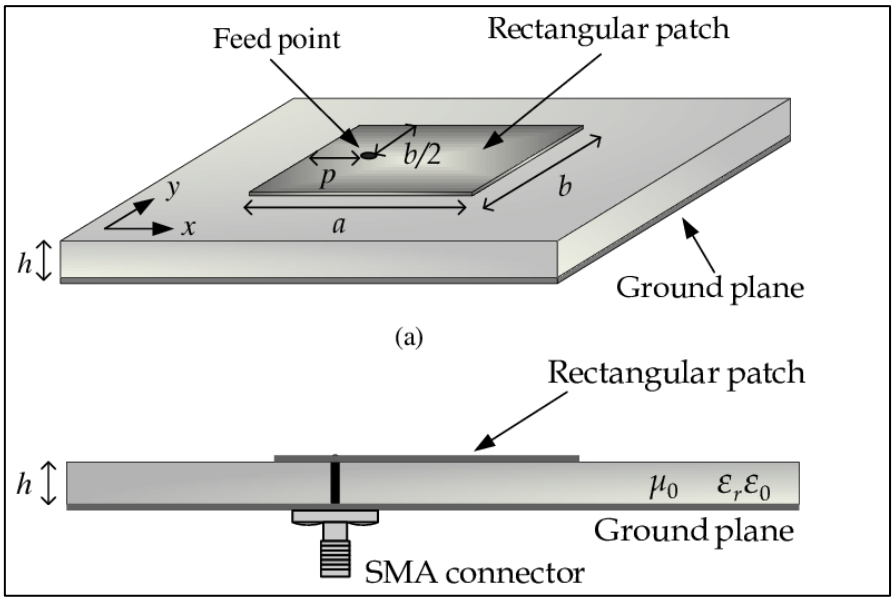

Figure 8: antenna with probe feeding model

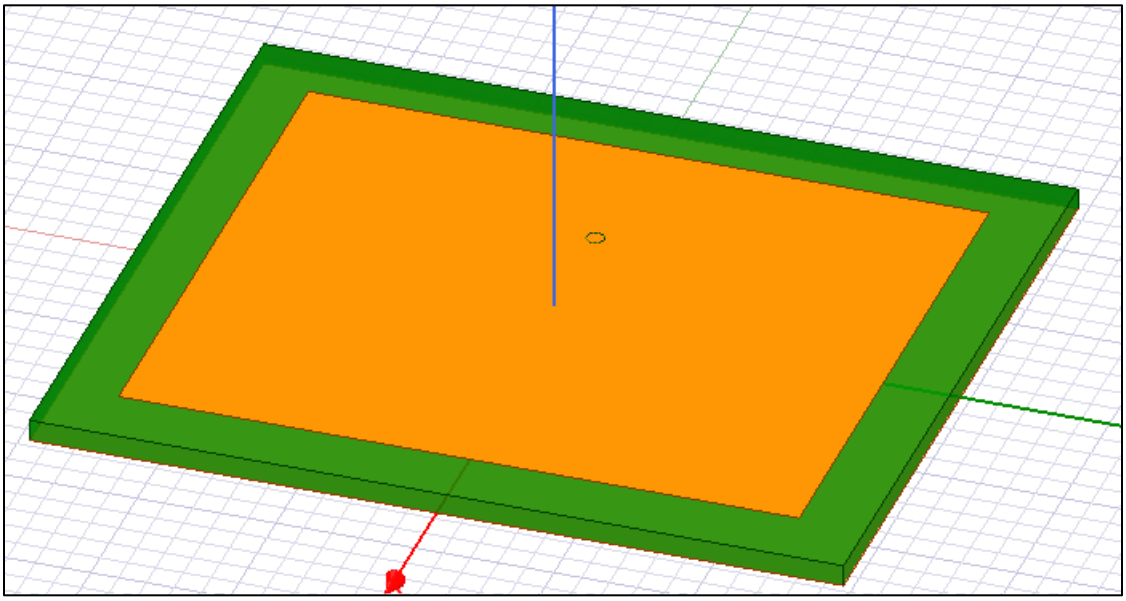

Figure 9: 3D patch antenna design

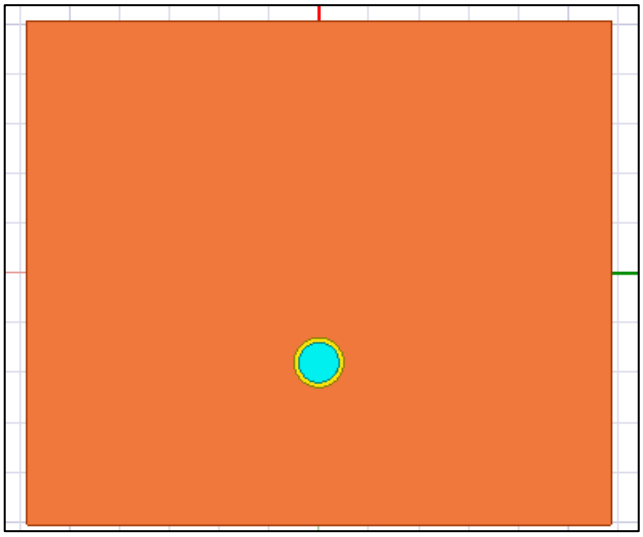

Figure 10: bottom view of patch antenna

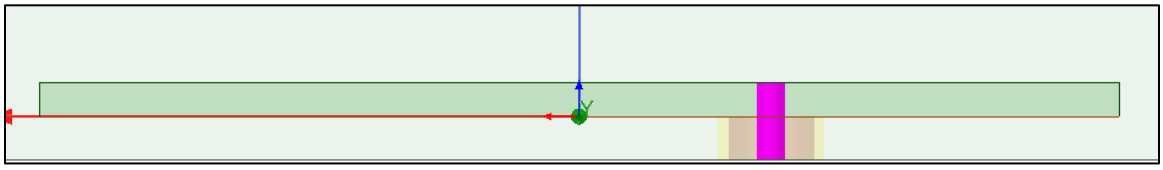

Figure 11: side view of patch antenna

And we designed and evaluated the values in Table 3:
The substrate length and width is designed so the patch has 3*hs in each side

Name	Unit	"Evaluated Value"	Description
Lp	Mm	3.633mm	Patch length
Wp	Mm	5.173mm	Patch width
hs	Mm	0.406mm	Substrate height
Ws	Mm	6*hs+Wp=7.609mm	Ground plane width
Ls	Mm	6*hs+Lp=6.475mm	Ground plane length
xfeed	Mm	1.2mm	Feed point x-offset
rcoax	Mm	0.14mm	Coaxial feed radius
hcoax	Mm	0.203mm	Coaxial feed height
rprope	Mm	0.07mm	Probe radius
Yfeed	Mm	0mm	Feed point y-offset
Hgnd	Mm	-0.032mm	Ground plane height

Table 3 Single Patch Design

S11:

For designing single patch antenna, we tuned parameters to get reflection coefficient S11 achieving specs

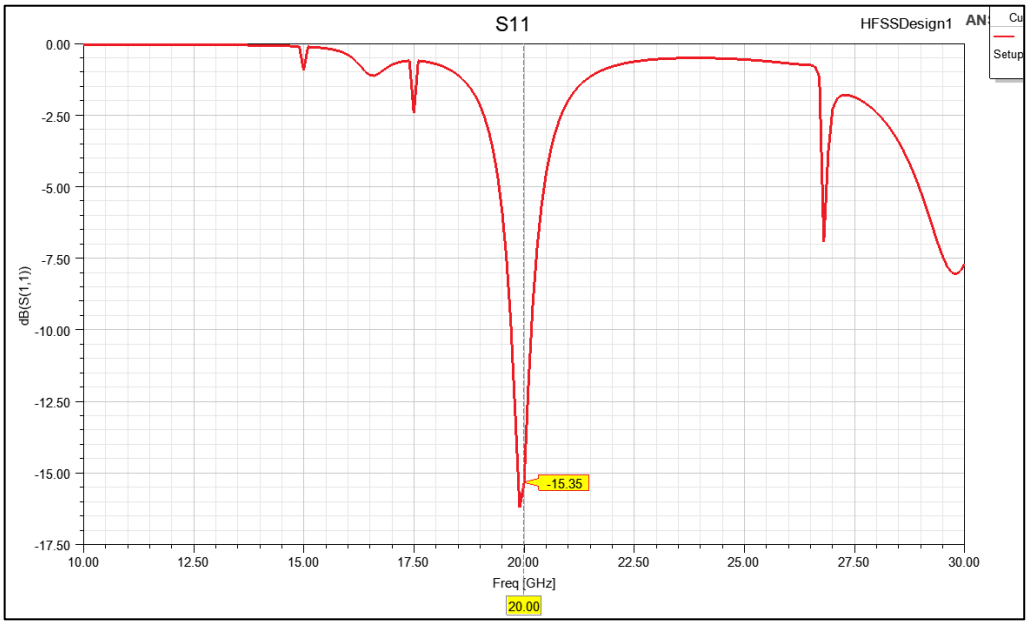

Figure 12: S11 for single Patch antenna

From figure 12, we succeeded to tuned parameters and achieve minimum s11 at operating frequency 20 GHz =-15.35dB

we have bandwidth (range of frequency where S11<-10 dB),The BW = 450 MHz.

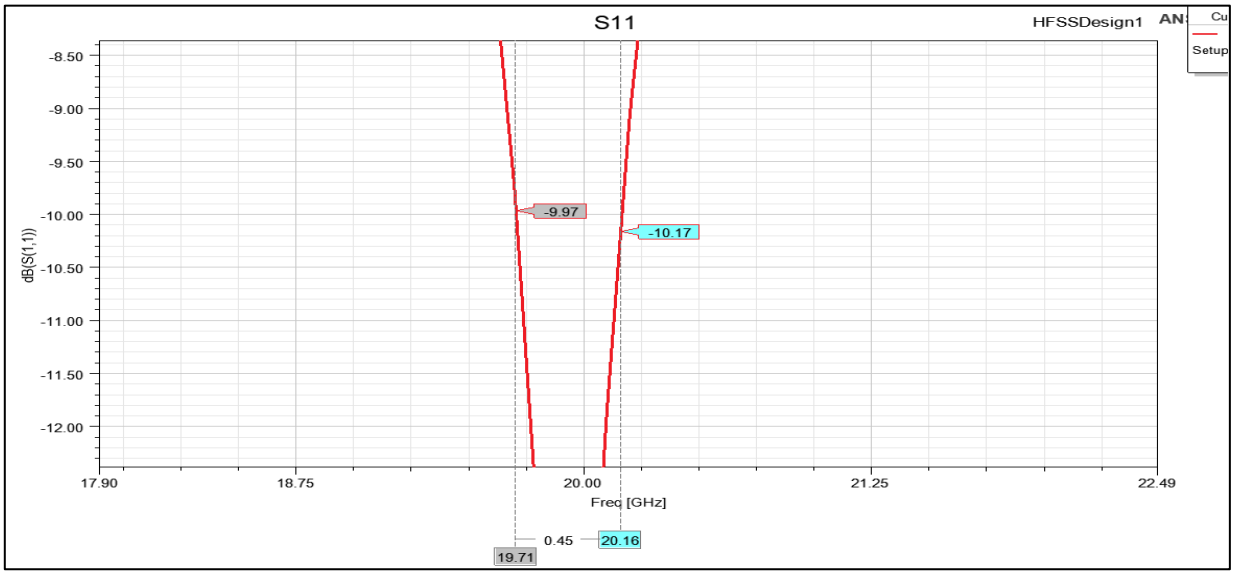

Figure 14: Bandwidth where S11<-10 dB

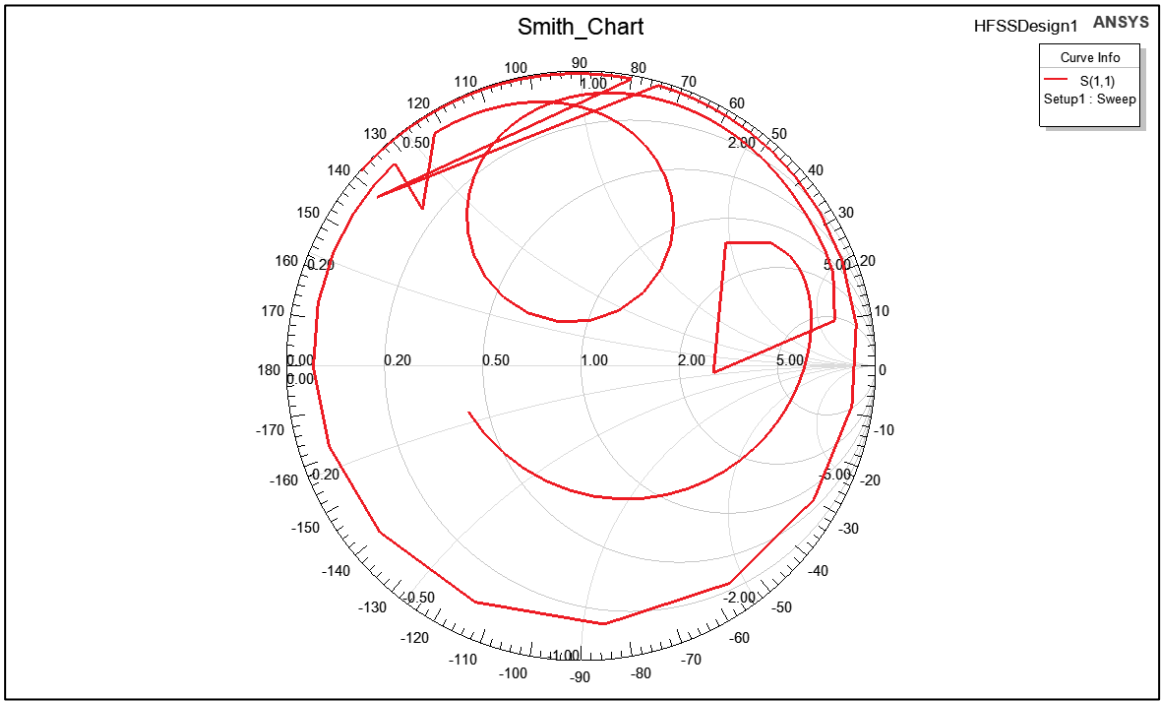

Figure 13: smith chart for single Patch

As shown in figure 15, Bandwidth achieved for VSWR=1.421

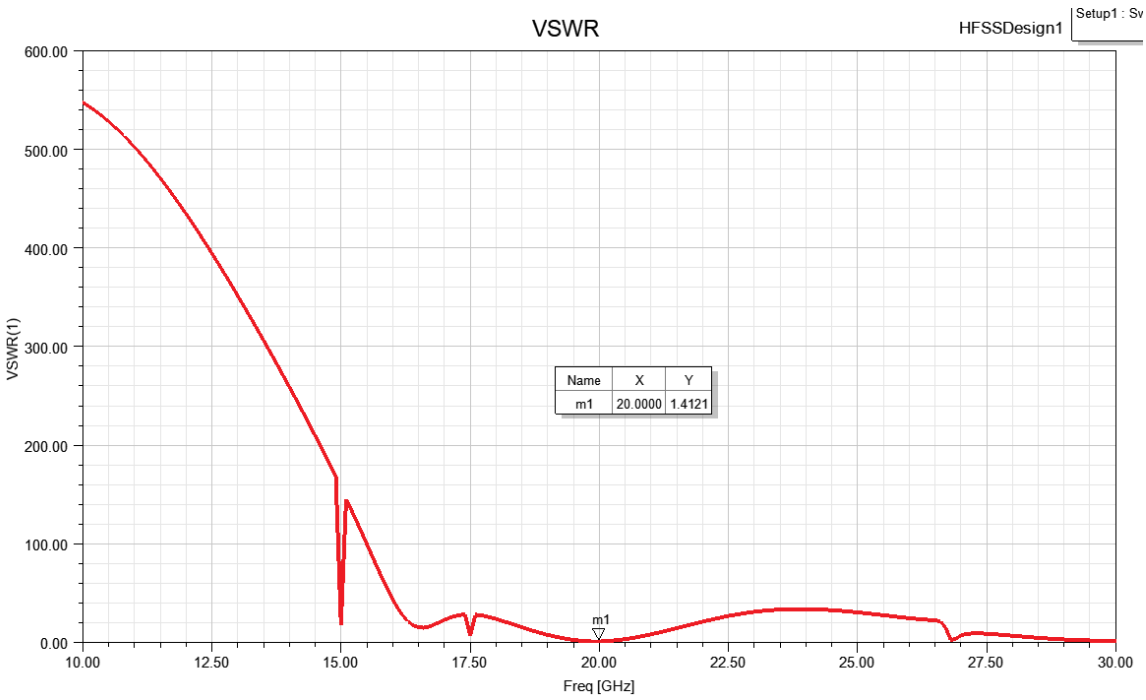

Figure 15: VSWR = 1.421 at 20 GHz for single patch antenna

Zin:

For proper feeding from the above figure 16, we found that $Zin = 40.74 + j\ 42.7$ is matching impedance required at 20GHz.

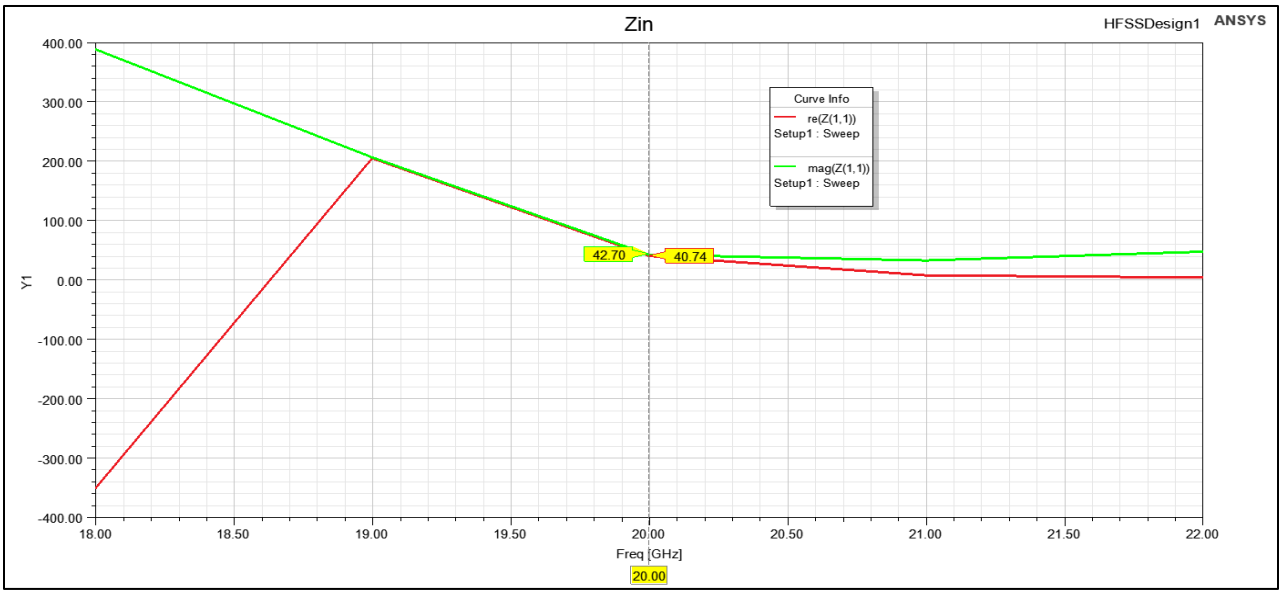

Figure 16 Zin for single Patch antenna at 20GHz

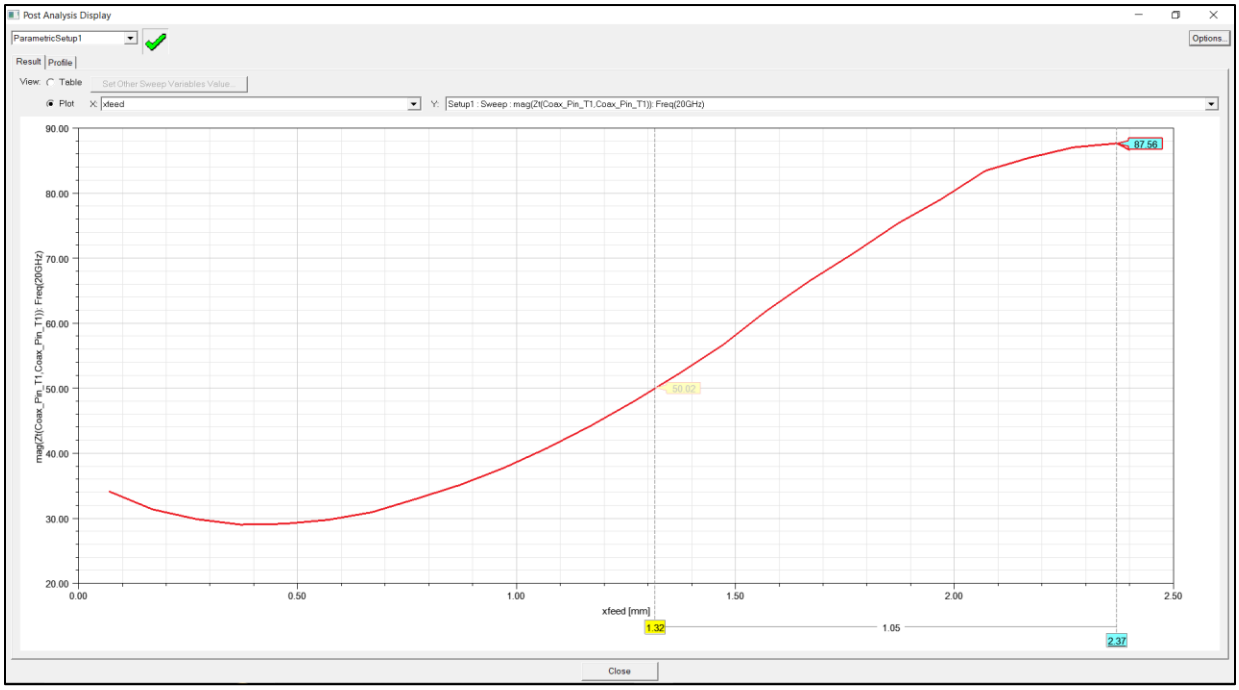

Figure 17 Xfeed for single patch antenna

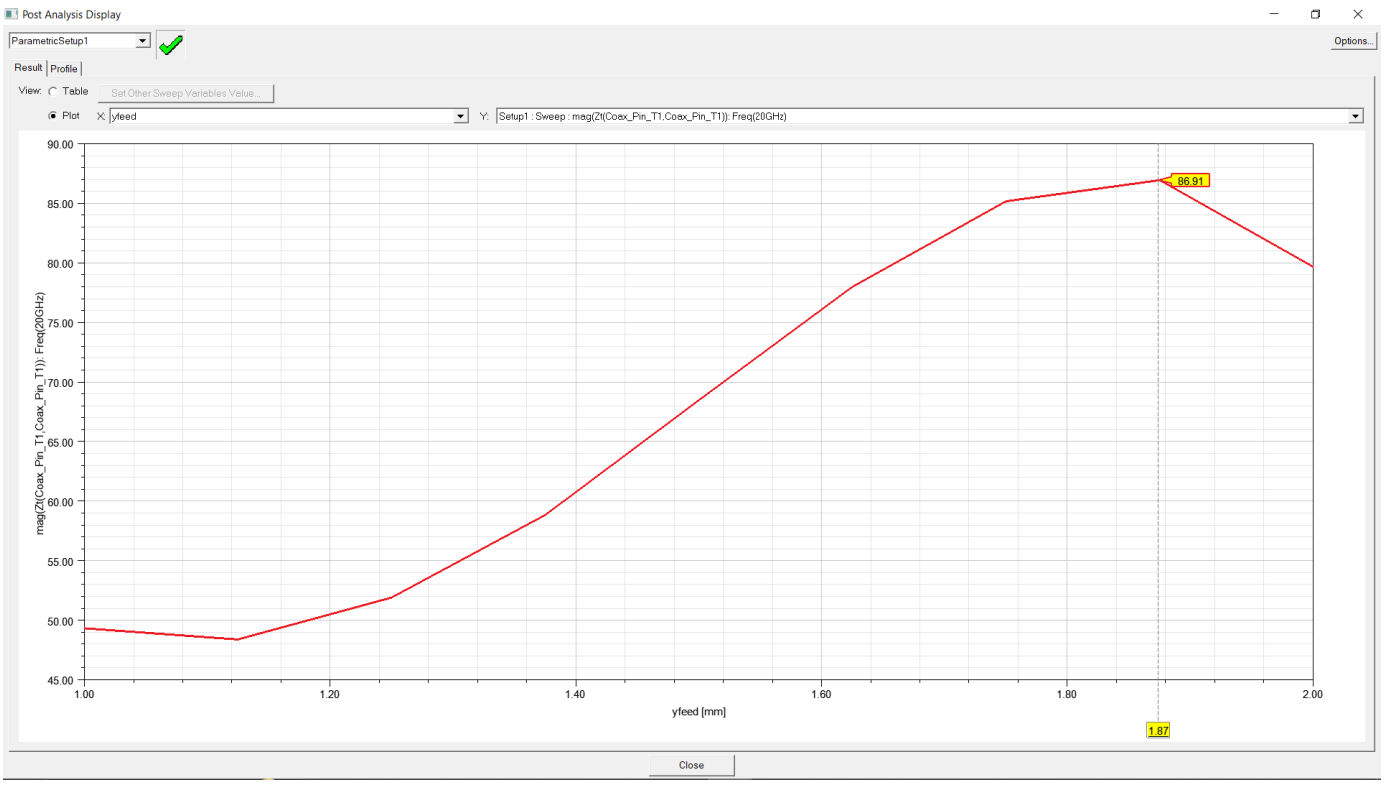

Figure 18: Yfeed for single patch antenna

From figure 17 and 18, We can see that (x,y) position can change the Zin value.

So we chose (1.2,0) that matched our specs.

Radiation patterns

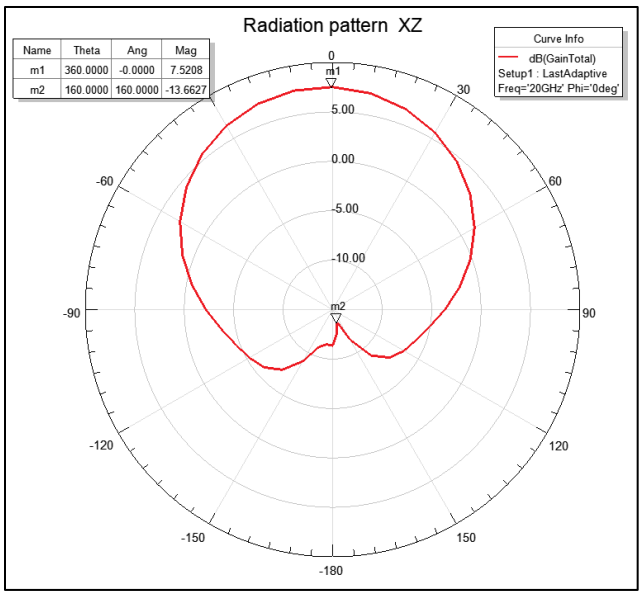

Figure 19 Radiation Pattern at 20GHz in XZ Plane

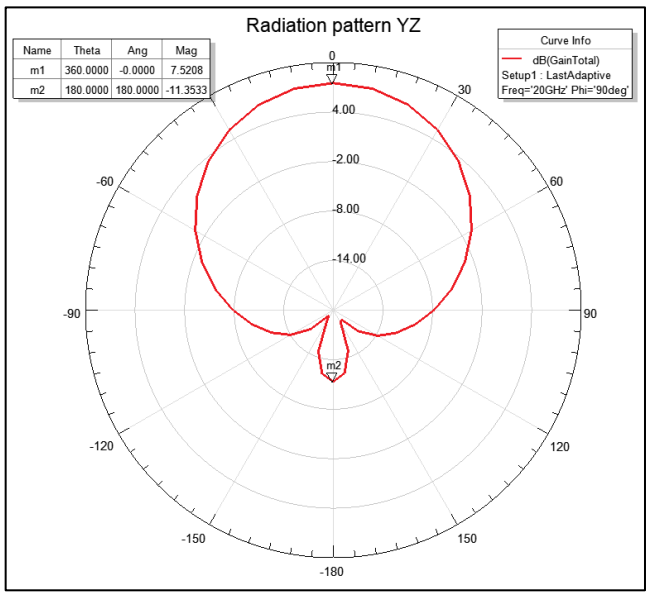

Figure 20 Radiation Pattern at 20GHz in YZ Plane

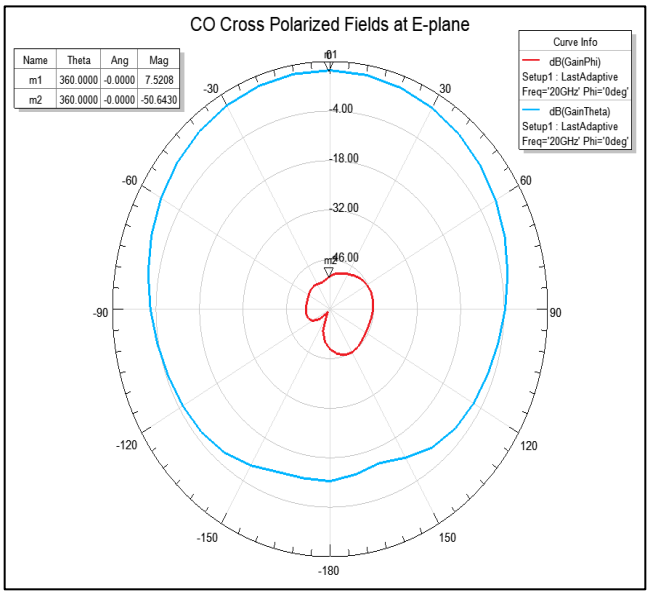

Figure 21 CO Cross Polarized Fields at E-plane

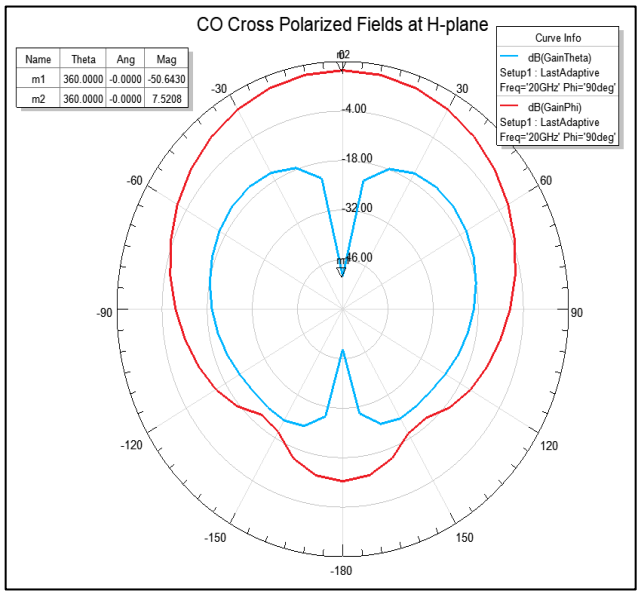

Figure 22 CO Cross Polarized Fields at H-plane

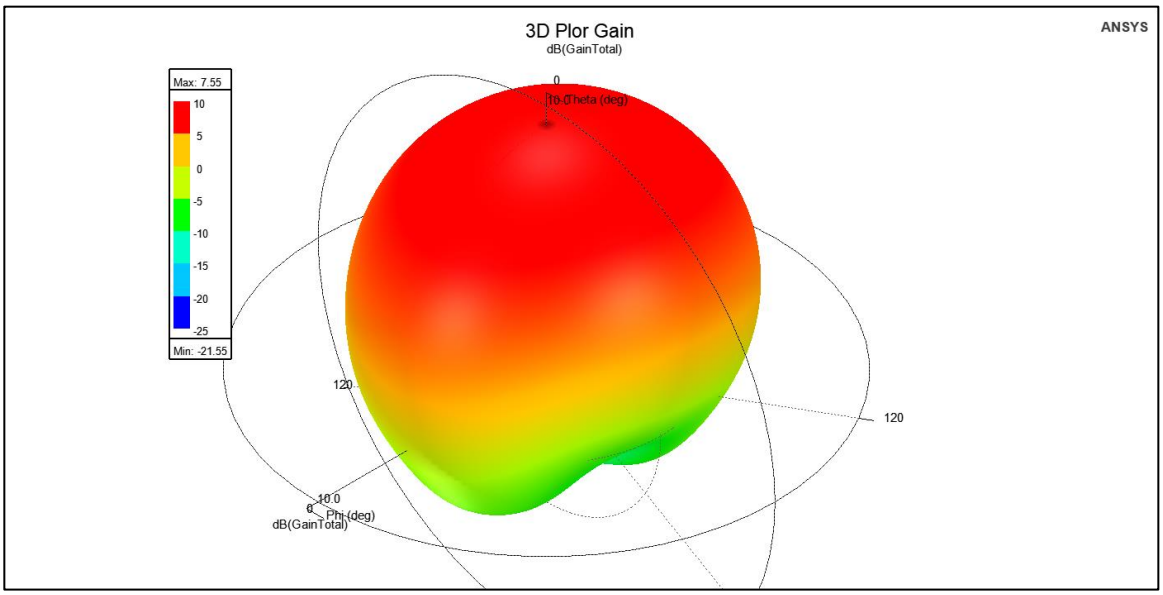

Figure 23 3D Polar Gain at 20GHz

Using the figures 19, 20, 21, 22 and 23, we can calculate the variables in Table 4:

Name	Evaluated Value
Gain	7.52dB
XPD	58.16dB
Front-to-Back$_{XZ}$	21.18dB
Front-to-Back$_{XY}$	18.87dB

Table 4 Single Patch Radiation Pattern Results

As shown in Figure 19 and Figure 20, the radiation pattern of the designed single antenna is illustrated along with the co- and cross-polarized fields. The antenna achieves a gain of 7.52 dB, indicating a strong directional performance. It can be observed from the co- and cross-polarization plots that the antenna achieves a high cross-polarization discrimination (XPD) of 58.16 dB, reflecting excellent polarization purity. Furthermore, the front-to-back ratio is 21.18 dB in the XZ plane and 18.87 dB in the XY plane, demonstrating good suppression of backward radiation and indicating stable performance across planes.

Antenna Parameters

	Freq [GHz]	RadiationEfficiency Setup1 : LastAdaptive	db(PeakGain) Setup1 : LastAdaptive
1	20.000000	0.958501	7.550215

Table 5 Single Antenna Parameters

The antenna gain is one of the key antenna characteristics as it combines radiation efficiency and directivity.

As shown in table 5, where the peak realized gain of the proposed antenna is 7.55 dB, indicating strong performance in the boresight direction. A radiation efficiency of 95.85% is achieved, showcasing the antenna's ability to efficiently convert input power into radiated energy. Note that this efficiency and gain are specific to the evaluated frequency range, as the simulation was focused on the design's target operational band.

Gain Performance of a Single Patch Antenna

As shown in Table 5, The gain of the single patch antenna was measured, and the results showed a single main beam centered at $\theta=0°$ with a maximum gain of 7.52dB and directivity of 7.7dB

This pattern is consistent with the fundamental radiation mode of a microstrip patch antenna, which is typically a broadside radiator designed to focus energy perpendicular to the patch surface.

The observed gain value of 5.7dB is within the expected range for a single patch operating at the designed frequency, accounting for the following factors:

1. **Effective Aperture:** The size and geometry of the patch contribute to its directivity.
2. **Substrate Material:** The dielectric constant and loss tangent of the substrate slightly influence the gain.
3. **Impedance Matching:** Proper matching ensures minimal reflection and maximum radiation efficiency.

This result establishes a baseline for evaluating the performance of the 2-element patch array configuration.

Design of Two Patches:

We are targeting to design 2 antenna arrays, so we made a replica from our patch and we swept and tuned our parameter to achieve the required specs

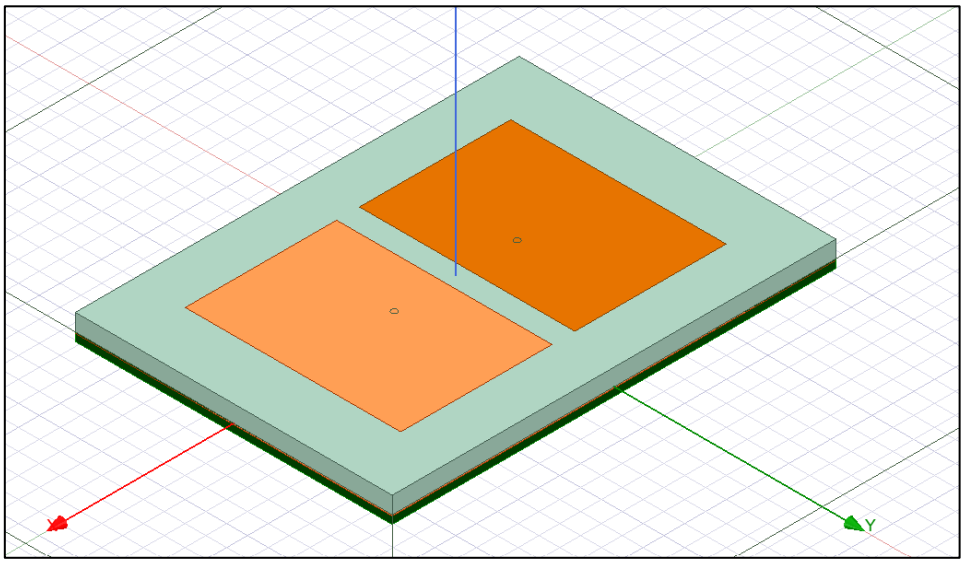

Figure 24: Two Patch antenna array

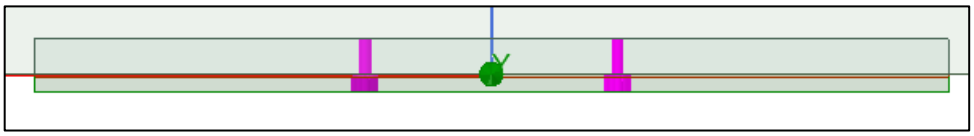

Figure 25: Two Patch side view

We make a sweap on distance between patches (dp) to meet the specs.

The best results was at dp=0.36mm putting in mind that it will change after designing the TL.

S-Parameters:

Also designing two patch antenna array is expected to provide us with higher gain compared to single patch however we noticed that there is a trade off between mutual coupling S21 and achieving required gain:

At first, we tuned parameters to achieve S11 as required

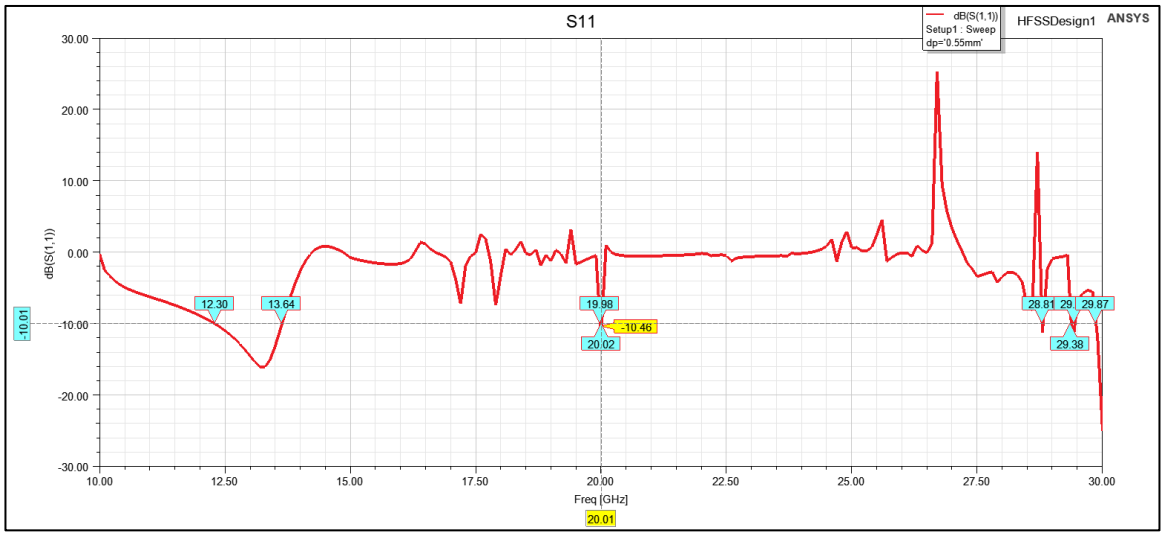

Figure 26: S11 for Two patches

As shown in Figure 26, We have S11 = -10.46 dB< -10 dB at 20 GHz however we faced problems with Bandwidth as it is a very narrow band.

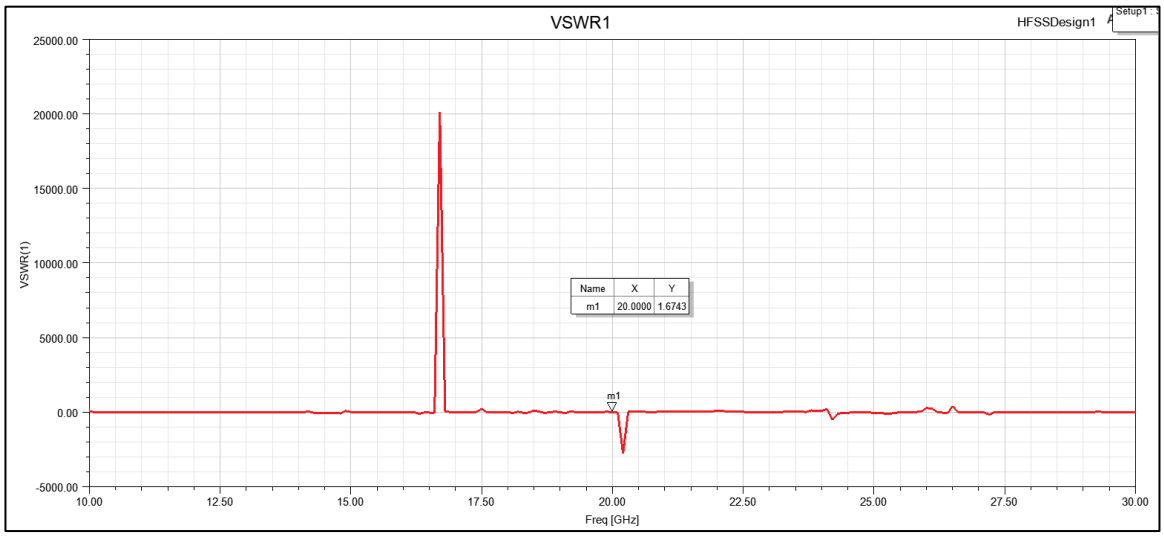

Figure 27: VSWR for first Patch

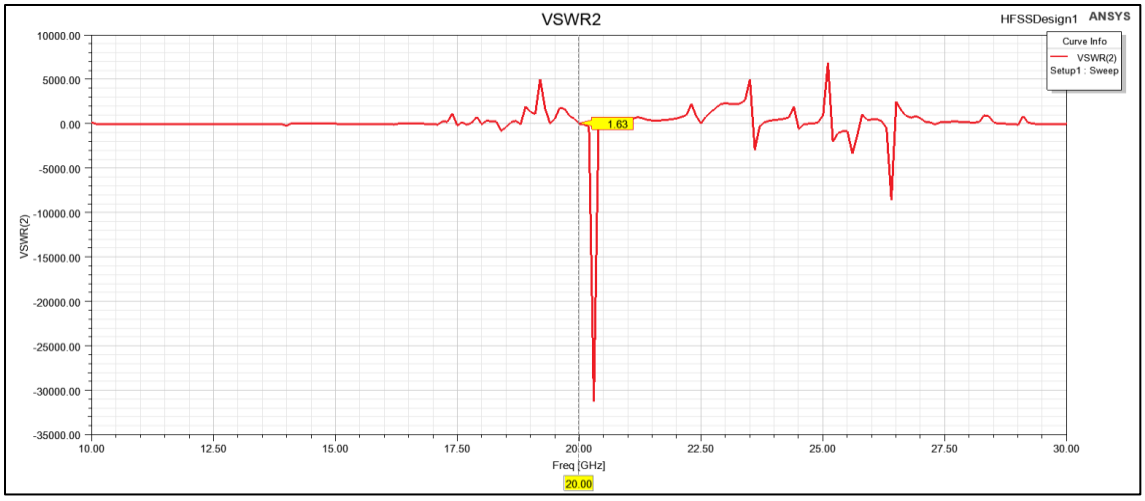

Figure 28: VSWR for second Patch

As shown in Figure 28 and 30, The VSWR1 VSWR2 is equal to 1.63.

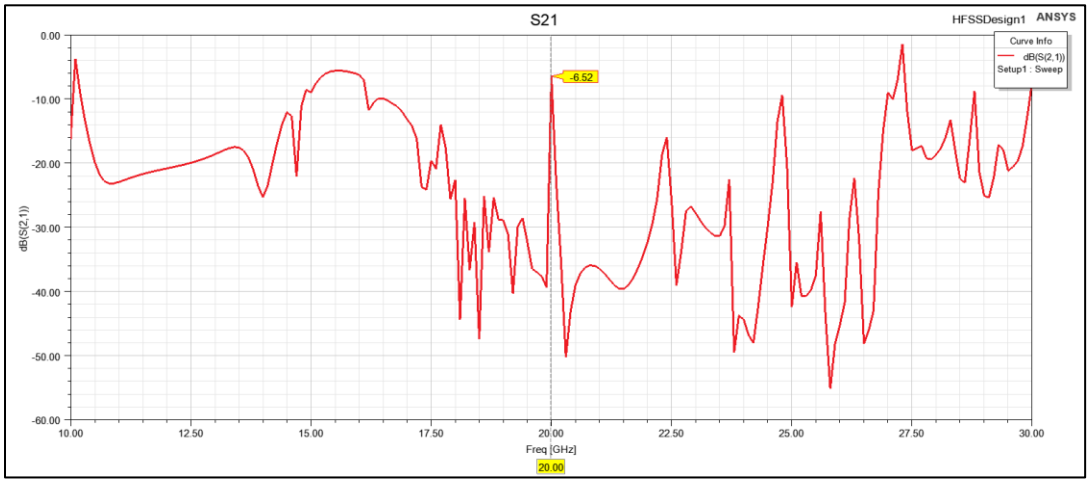

Figure 29: S21 Vs Frequency

As shown in figure 29, The S21 value equals to -6.52 dB.

Mutual Coupling vs Element Spacing:

as we discussed mutual coupling S21 originated when we add the second patch and we noticed that it varies with distance between two patches (dp) so we made sweep on:

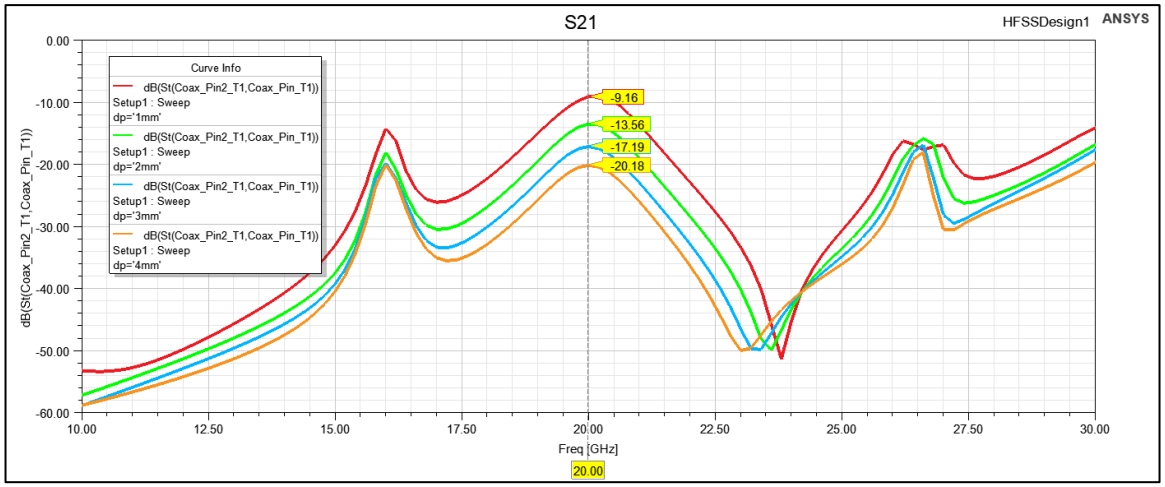

Figure 31: S21 sweep Vs frequency by changing dp

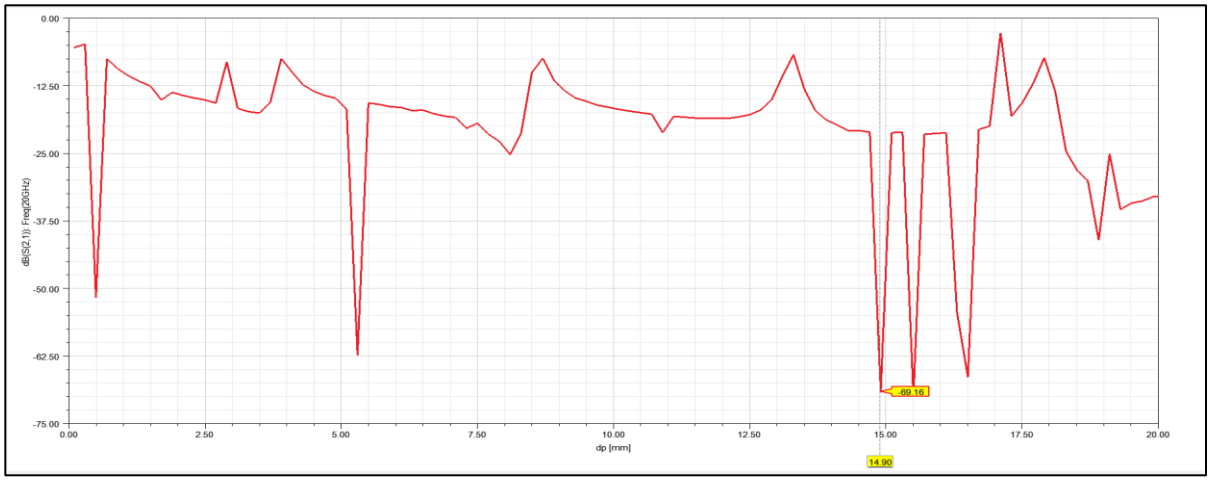

Figure 30: S21 Vs Distance between two patches swept till λ

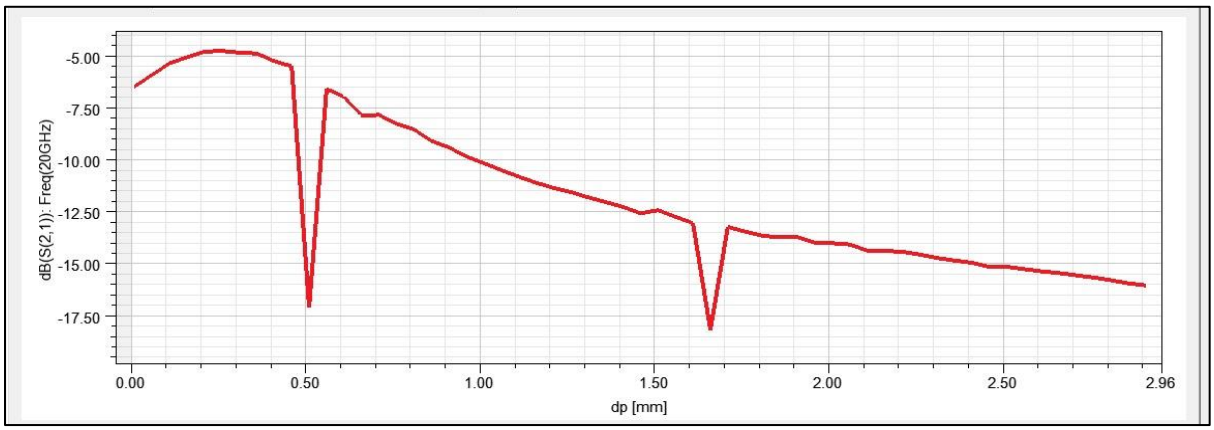

Figure 32 S21 Vs Element Distance on small scale

As shown in figure 30 and 32:

The behavior of the S21 graph versus element distance is primarily due to the constructive and destructive interference of the electromagnetic waves radiating from the two patches.

At certain distances, the waves reinforce each other, creating tops in the graph, while at others, they cancel out, resulting in bottoms. These interactions are influenced by the phase difference between the signals from the patches, which changes with element spacing.

The observed tops at 8.7 mm, 13.31 mm, and 17.11 mm correspond to distances where the phase alignment of the waves maximizes coupling. Conversely, the bottoms at 14.9 mm, 15.5 mm, and 16.5 mm represent destructive interference points where the coupling is minimized with S21 = -70 dB.

We will choose for the TL design a distance of based on sweaping with the TL

Zin:

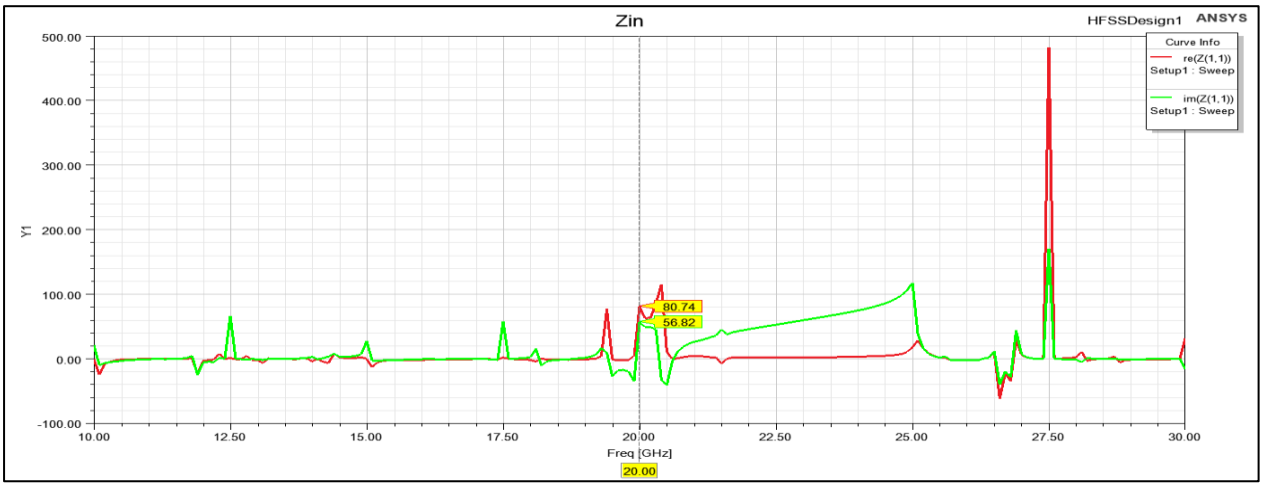

Figure 33: Zin for two Patches at 20 GHz

As shown in figure 33, The Zin equals to 80.74 + j 56.82 Ω

We got Zin=69.05 so for proper feeding and enhancing bandwidth.

Radiation patterns

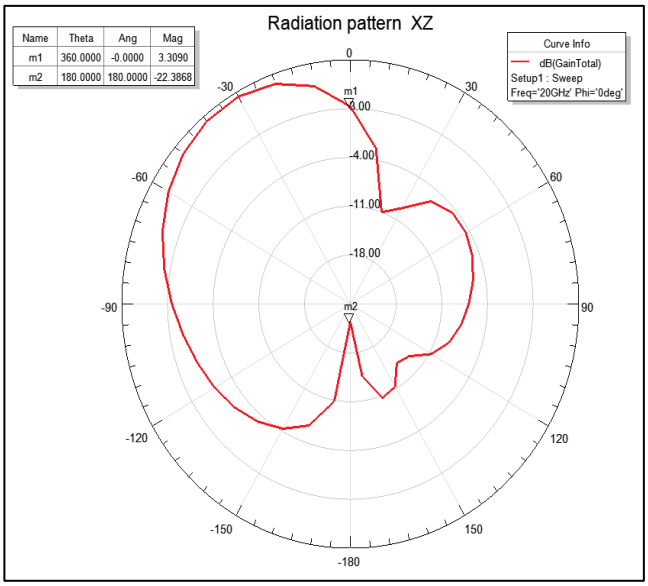

Figure 35 Radiation Pattern at 20GHz in XZ Plane

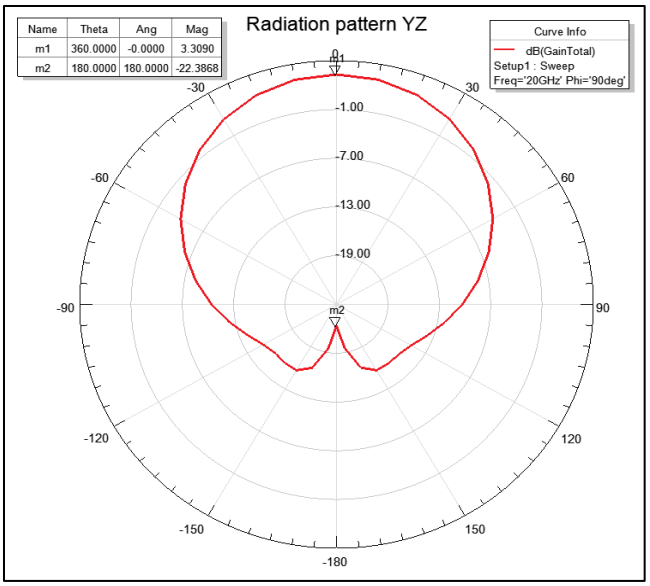

Figure 34 Radiation Pattern at 20GHz in YZ Plane

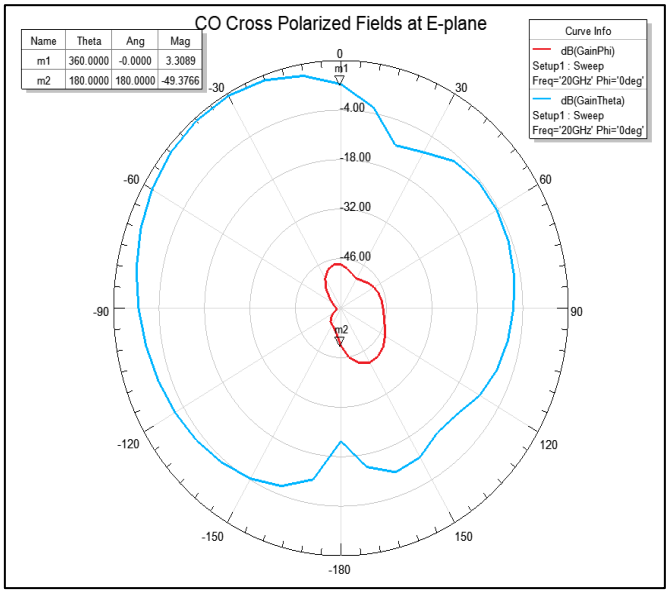

Figure 36 CO Cross Polarized Fields at E-plane

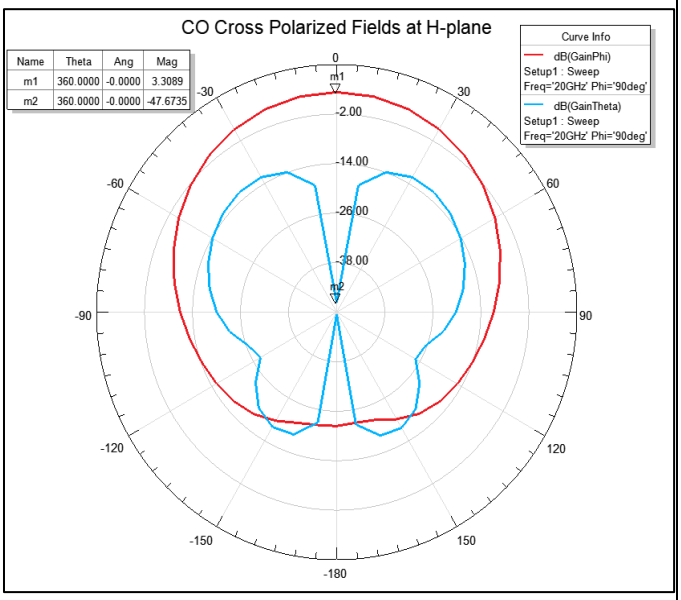

Figure 37 CO Cross Polarized Fields at H-plane

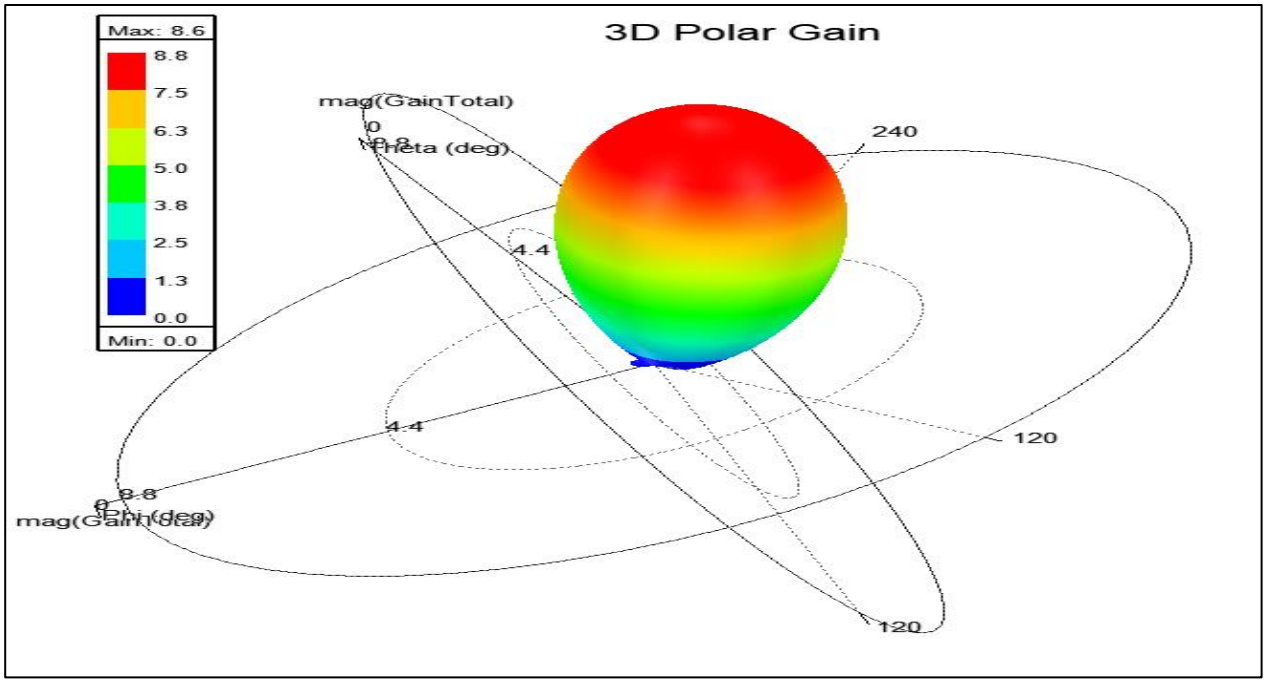

Figure 38 3D Polar Gain at 20GHz

Using the figures 35, 36 ,37 and 38, we can calculate the variables in Table 6:

Name	Evaluated Value
Gain	3.3dB
XPD	52.67dB
Front-to-Back$_{XZ}$	25dB
Front-to-Back$_{XY}$	25dB

Table 6 Two Patch Radiation Pattern Results

As shown in Table 6, when the two patches were combined into an array, the mutual coupling between the elements and the phase difference between their feeds caused the main lobe of the radiation pattern to shift, with the main beam centered at θ = -30°. This offset, typical of such interactions, arises from unequal phase distribution or asymmetry in the feed network.

The array achieved a gain of 3.3 dB and a cross-polarization discrimination (XPD) of 52.67 dB, with a front-to-back ratio of 25 dB in both the XZ and XY planes, as summarized in Table 6. However, the radiation efficiency was lower than that of the single patch due to the offset and coupling effects, highlighting the trade-off between gain improvement and efficiency in array configurations.

This behavior can be attributed to the following factors:

1. **Element Spacing and Phase Difference:**
    - The mutual coupling and spacing between the two patches likely introduced a phase difference in the radiated fields from each element. This phase offset caused constructive interference to occur at an angle rather than directly broadside (θ=0∘\theta = 0^\circθ=0∘).
2. **Feed Network Asymmetry:**
    - If the feed network introduced a phase imbalance between the two patches, it would steer the beam away from the broadside direction.
3. **Mutual Coupling Effect:**
    - The interaction between the two patches may have modified the effective radiation pattern, pushing the main beam off-center.

This result highlights the importance of ensuring symmetrical feeding and carefully managing element spacing to maintain broadside radiation. Corrective measures, such as tuning the transmission line lengths or adjusting the relative phases, can mitigate this offset.

Antenna parameters:

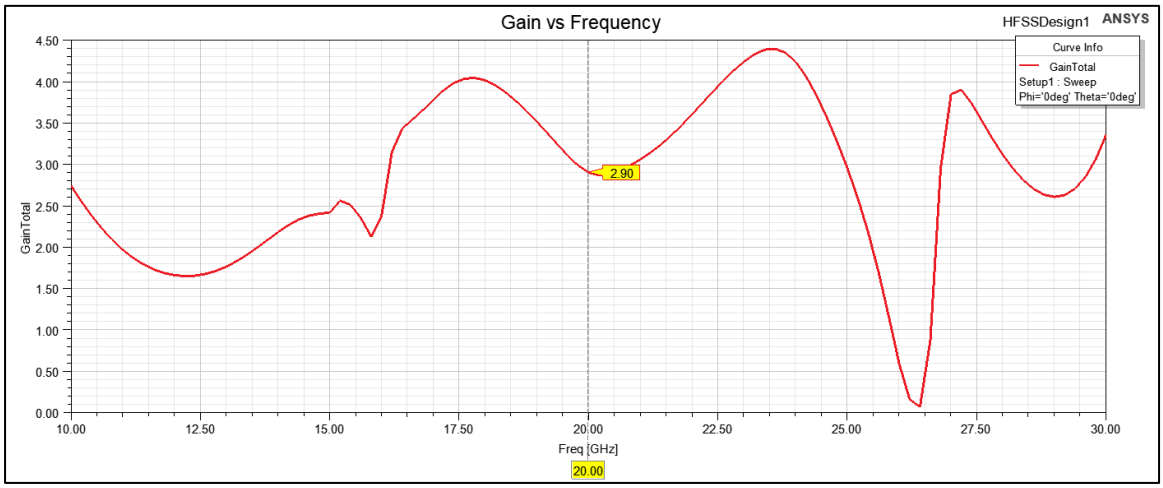

Figure 39 Two Patch Gain Vs Frequency

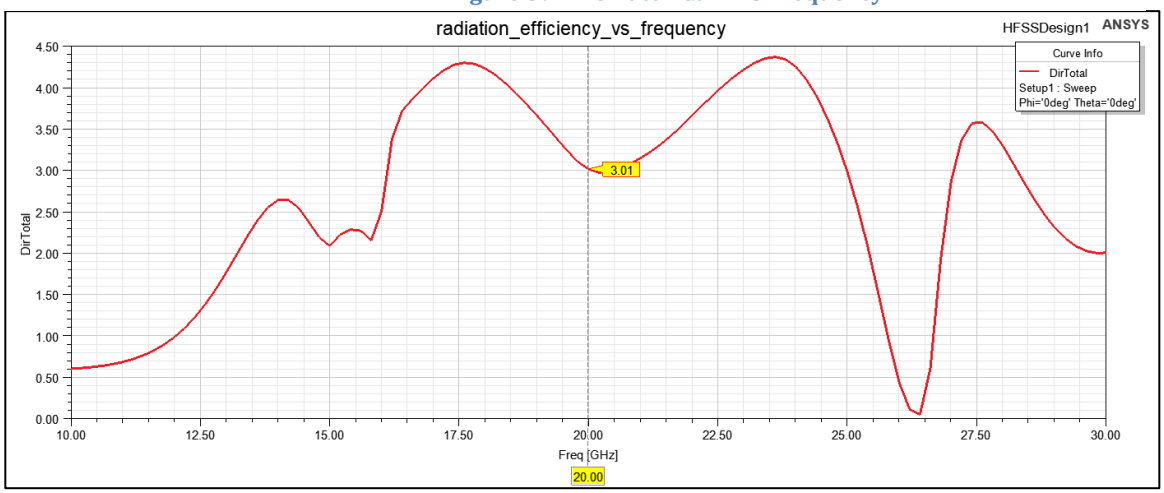

Figure 40: Radiation Efficiency Vs Frequency

As shown in figure 39 and 40, The plots of **Gain** and **Radiation Efficiency** versus frequency for the two-patch array reveal the following observations:

1. **Maximum Gain and Efficiency:**

   - The total gain reaches 9.2dB and radiation efficiency peaks at 9.57dB, but these values are not the global maxima across the frequency range.

2. **Two Distinct Peaks:**

   - The gain and efficiency curves exhibit two prominent peaks at approximately **17.5 GHz** and **23.5 GHz**, indicating the frequencies where the array's performance is optimized.
   - These peaks could be attributed to **resonances** of the patches, where the radiation is most efficient due to better impedance matching and minimal losses.

3. **Behavior Between Peaks:**

- Between these peaks, the gain and efficiency slightly drop, likely due to suboptimal matching or increased losses in the antenna system.

To maximize performance at a specific operational frequency, the design could be further tuned, such as by adjusting the element spacing, feed network, or patch dimensions. Including this analysis in the report emphasizes the importance of frequency optimization in array design.

Adding Feeding Network for Two Patch antennas:

Serial Transmission Line:

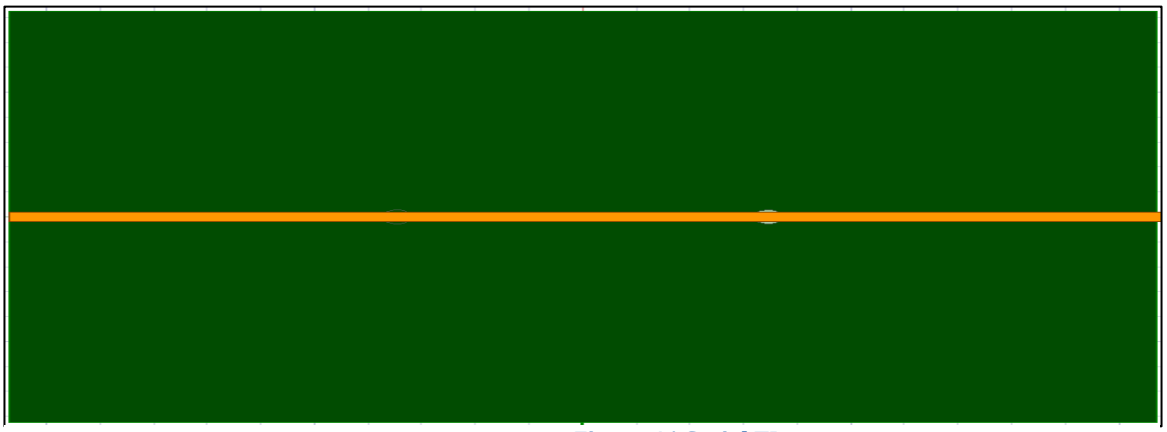

Figure 41 Serial TL

As shown in figure 41, We first tried to use the Serial TL with the Two patches with dimensions in Table 7:

Name	Unit	"Evaluated Value"	Description
LTL_feed	mm	Ls=10.72mm	Feed transmission line length
WTL_feed	mm	0.3mm	Feed transmission line width

Table 7 Serial TL Dimensions

Results:

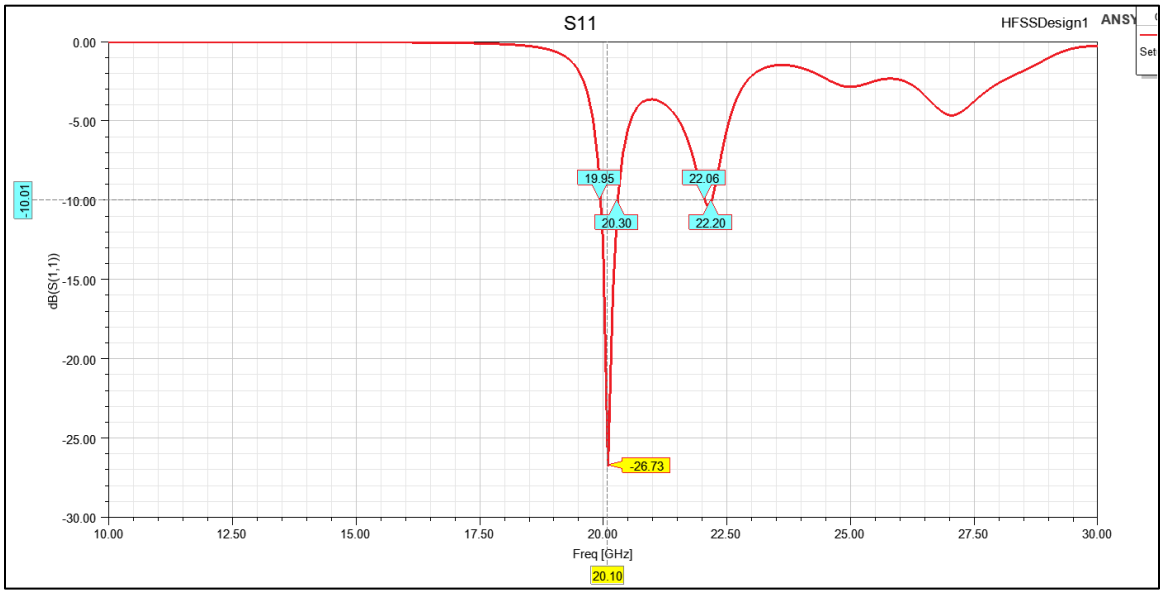

Figure 42 S11 with Serial TL

As shown in figure 42, The S11 achieved the specs

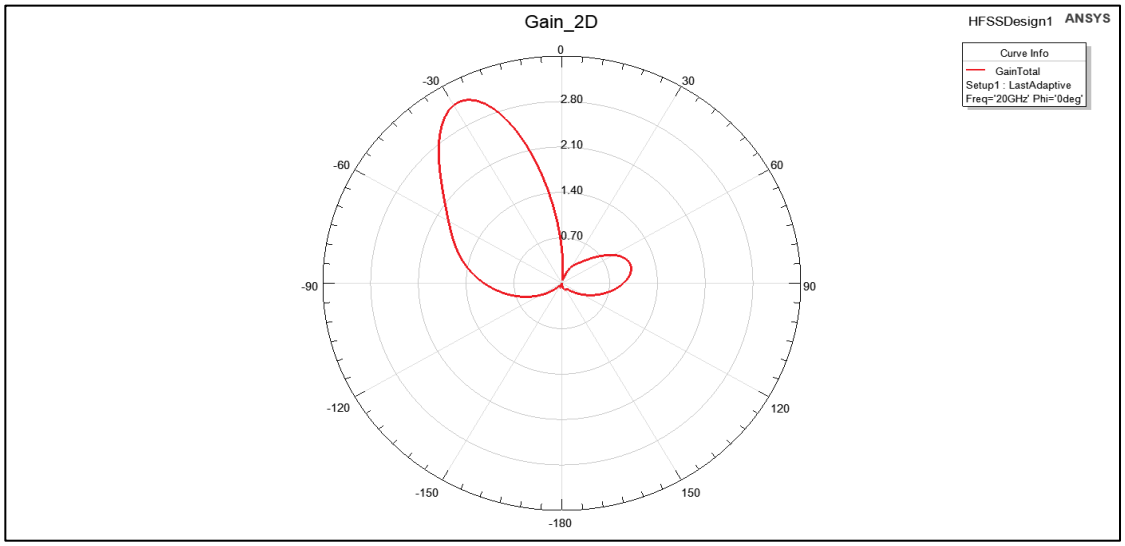

Figure 43 Gain with Serial TL

As shown in figure 43, The gain was centered at θ =−30°.

The serial transmission line improved impedance matching (S11), but the radiation pattern remained centered at θ = -30° due to phase imbalance between the two patches, caused by unequal path lengths. This imbalance led to constructive interference in the offset direction.

So we shifted to T-section design

Final Design with T-Section Transmission Line:

As shown in figure 44, We designed a transmission line T-section as shown below and we swept on its dimensions till we achieved requirement.

And to have maximum gain we make distance equal to **λ = 15mm**

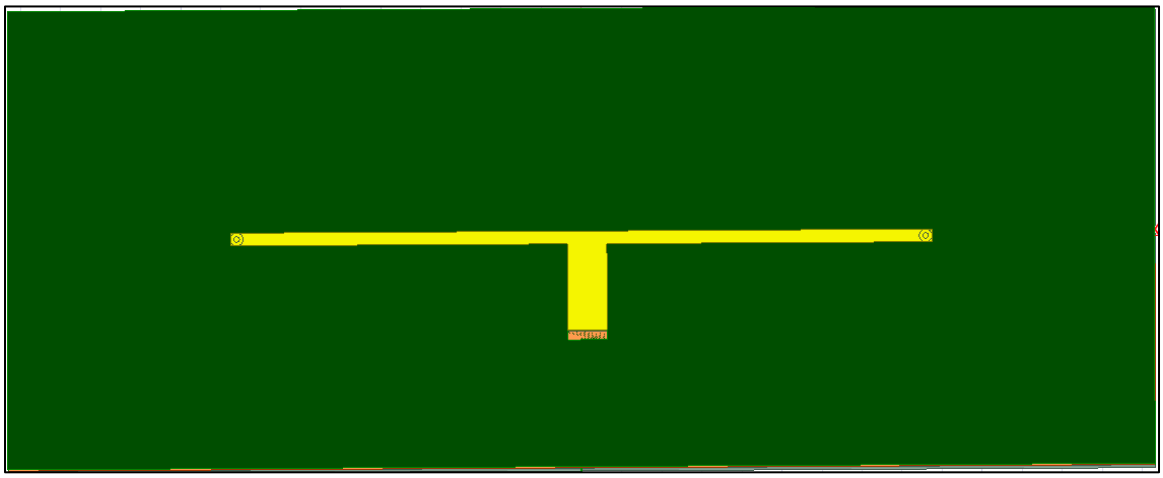

Figure 44: T-Section transmission line

After Sweaping, The final dimensions are in Table 8:

Name	Unit	Evaluated Value	Description
Lp	mm	5.78mm	Patch length
Wp	mm	7.54mm	Patch width
hs	mm	0.406mm	Substrate height
Ws	-	11.736mm	Ground plane width
Ls	-	18.206mm	Ground plane length
xfeed	mm	1.1mm	Feed point x-offset
dp	mm	3.5mm	Patch offset parameter
rcoax	mm	0.16mm	Coaxial feed radius
hcoax	mm	0.203mm	Coaxial feed height
rprope	mm	0.07mm	Probe radius
yfeed	mm	0mm	Feed point y-offset
hgnd	mm	-0.032mm	Ground plane height
Xcoax	-	2	Coaxial feed x-offset
WTL_In	mm	0.673367mm	Input transmission line width
LTL_feed	mm	2.179292mm	Feed transmission line length
WTL_feed	mm	0.976256mm	Feed transmission line width
LTL_Slot	mm	0.25mm	Slot length

Table 8 Final Design

S11:

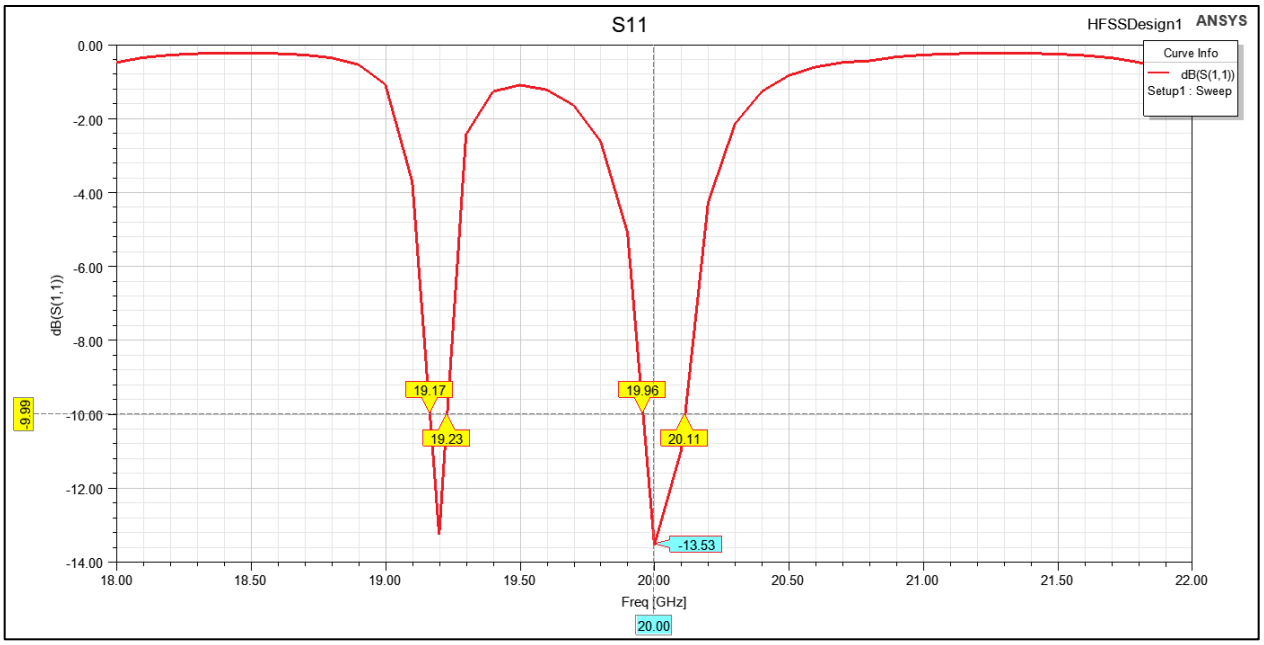

Figure 45: S11 after adding T-section

From figure 45, we enhanced bandwidth to be more wide from 19.96 GHz to 20.11 GHz with BW= 150MHz.

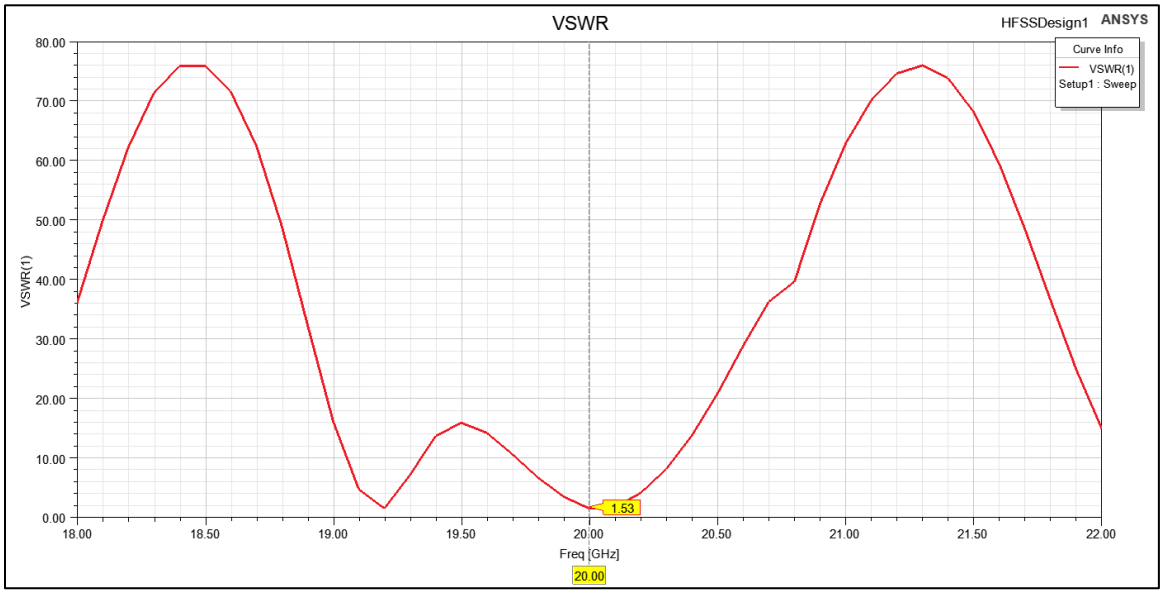

Figure 46: VSWR after adding feeding network

As shown in figure 46, The VSWR at frequency 20Ghz equals to 1.33.

Zin:

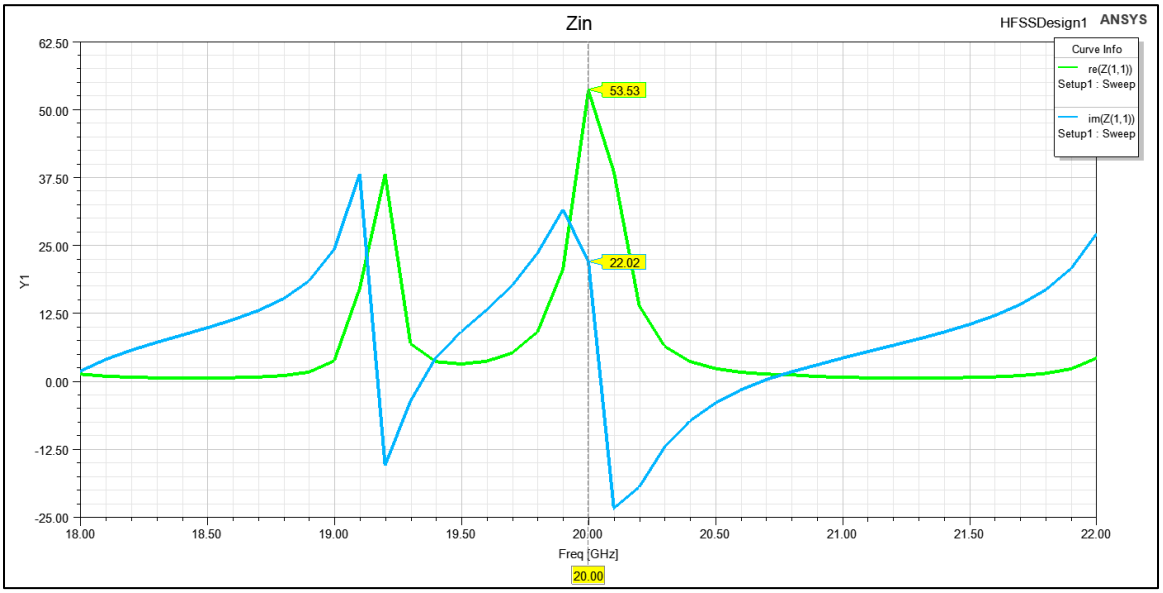

Figure 47: Zin after adding T-section transmission line

As shown in figure 47**,** the input**.53 + j22.02 Ω**. The resistive component **53.53 Ω** indicates a good match to the standard 50 **Ω** feed line, minimizing reflection losses. However, the reactive component **+j22.02 Ω** suggests the presence of inductive reactance, which could lead to impedance mismatch if not compensated. Proper matching techniques, such as using a matching network or adjusting the antenna geometry, may be required to achieve a purely resistive impedance for optimal power transfer.

Radiation patterns

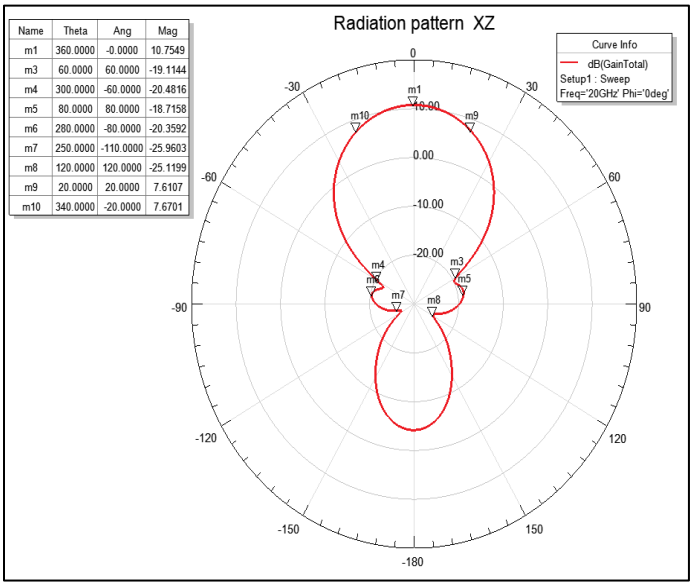

Figure 48 Radiation Pattern at 20GHz in XZ Plane

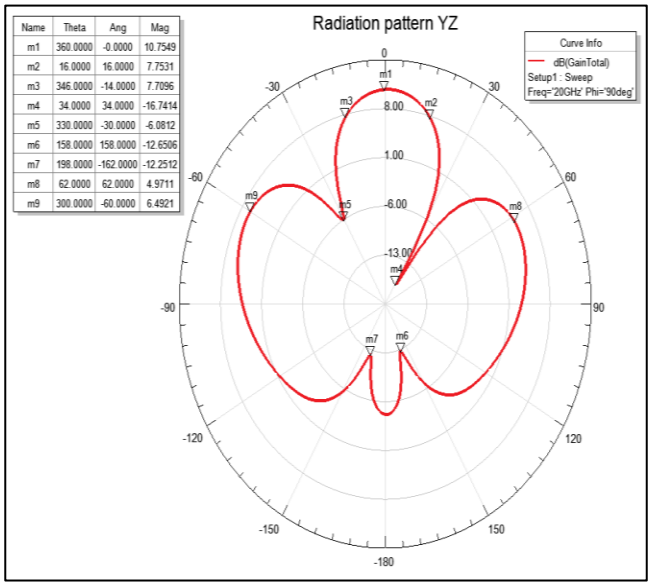

Figure 49 Radiation Pattern at 20GHz in YZ Plane

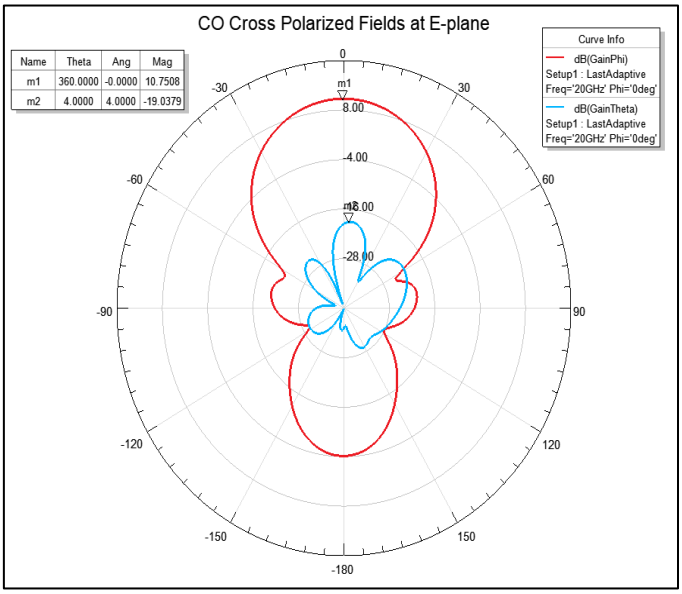

Figure 50 CO Cross Polarized Fields at E-plane

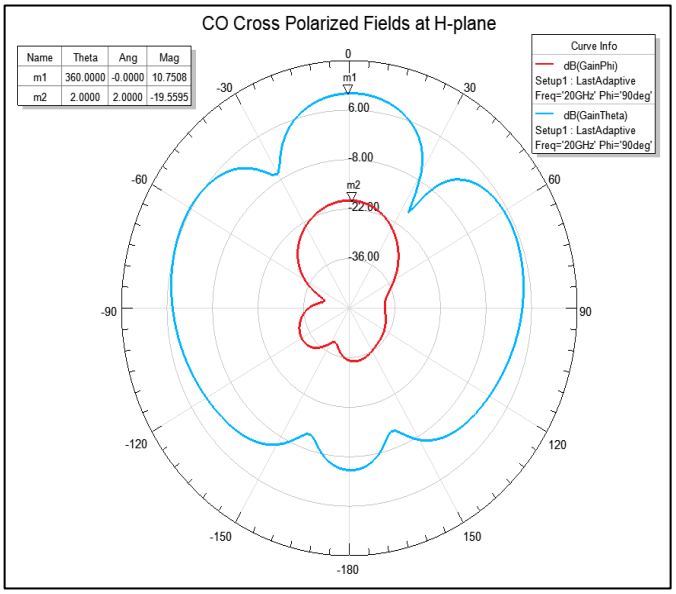

Figure 51 CO Cross Polarized Fields at H-plane

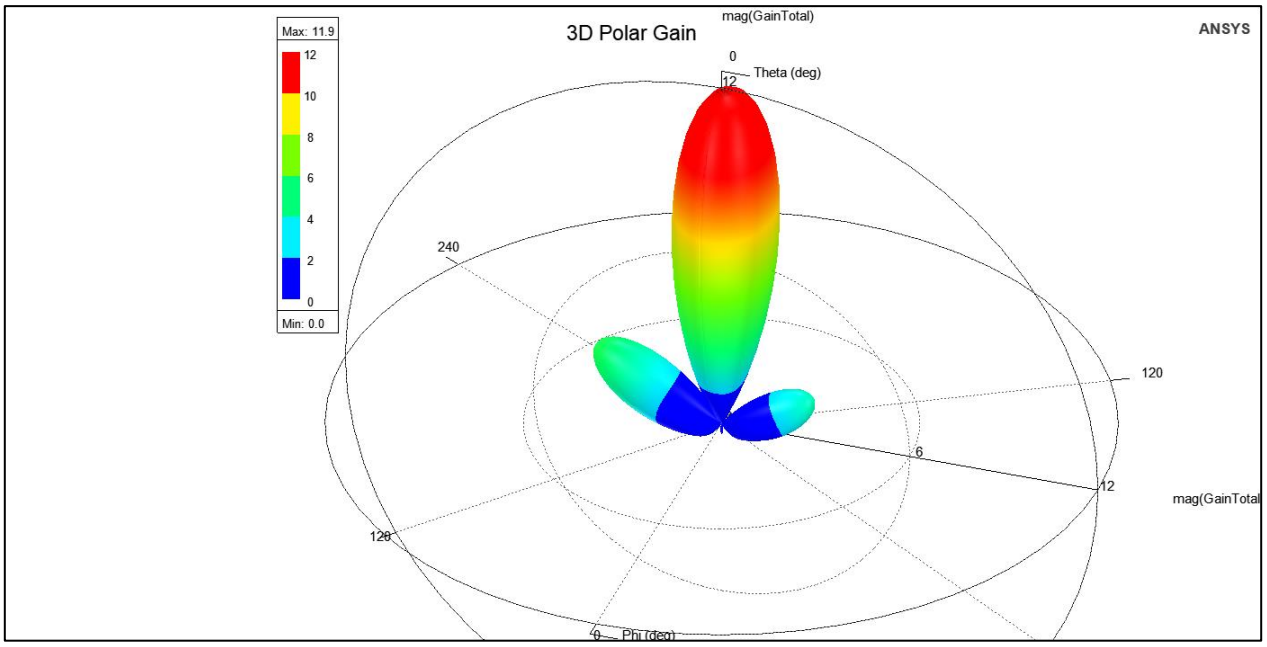

Figure 52 3D Polar Gain at 20GHz

Using the figures 48, 49, 50, 51 and 52, we can calculate the variables in Table 9:

Name	Evaluated Value
Gain	10.75dB
XPD	29.78dB

Table 9 Final Two Patch Radiation Pattern Results

As shown in the Table 9, the addition of the T-section transmission line effectively corrected the radiation pattern alignment. This adjustment centered the pattern at theta equal to zero, addressing the previous deviation observed at -30 degrees. The T-section design improved the impedance matching, ensuring proper energy distribution and pattern symmetry.

Beamwidth:

Using figure 49, We calculated the XZ beams in Table 10:

Name	Evaluated Value
Gain	10.75 dB
3dB beamwidth	40°
Fisrt Null beamwidth	120°
First Null	60°
Side Lobe beamwidth	60°
Side Lobe	80°

Table 10 XZ Beamwidth

Using figure 50, We calculated the XY beams in Table 11:

Name	Evaluated Value
Gain	10.75 dB
3dB beamwidth	32°
Fisrt Null beamwidth	64°
First Null	30°
Side Lobe beamwidth	124°
Side Lobe	62°

Table 11 XY Beamwidth

As shown in **Figure 49**, the beamwidth parameters in the XZ plane were evaluated and tabulated in **Table 10**. The antenna exhibits a gain of **10.75 dB**, a **3dB beamwidth** of **32°**, and a **First Null Beamwidth** of **64°** with the first null occurring at **30°**. Additionally, the **Side Lobe Beamwidth** was measured at **124°**, and the **Side Lobe Level** was **62°**. These values reflect the antenna's sharp directivity and controlled sidelobe levels in the XZ plane.

Similarly, as shown in **Figure 50**, the beamwidth parameters in the XY plane were evaluated and presented in **Table 11**. The gain remains at **10.75 dB**, with a **3dB beamwidth** of **40°**, a **First Null Beamwidth** of **120°**, and the first null occurring at **60°**. The **Side Lobe Beamwidth** in the XY plane was **60°**, and the **Side Lobe Level** was observed at **80°**.

The differences between the XZ and XY plane beamwidths highlight the directional variations in the radiation pattern, which are influenced by the antenna's design and mutual coupling effects.

Gain:

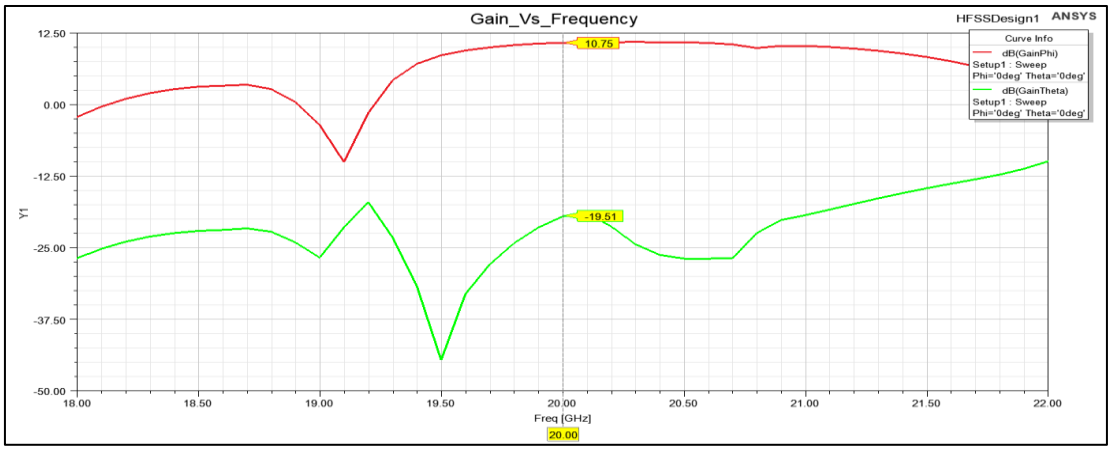

Figure 55 Gain Vs Frequency

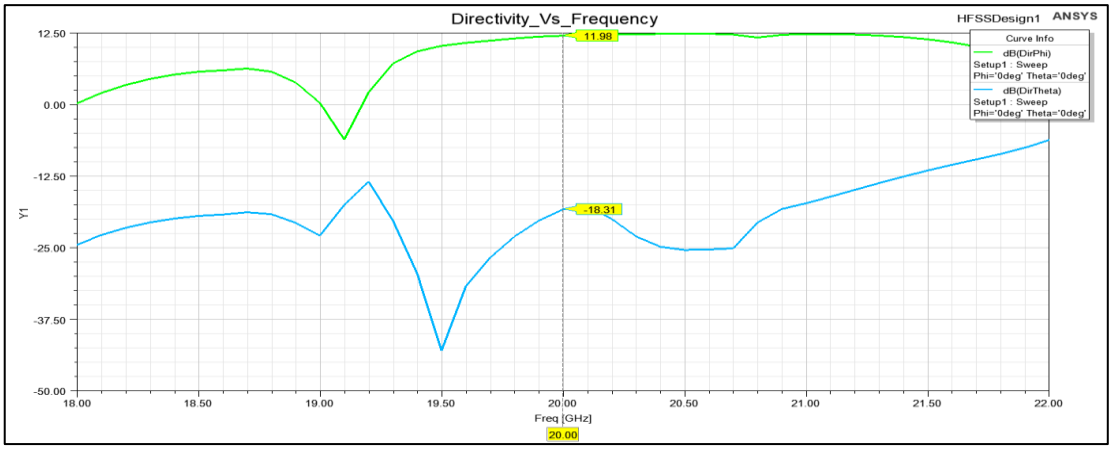

Figure 54 Directivity Vs Frequency

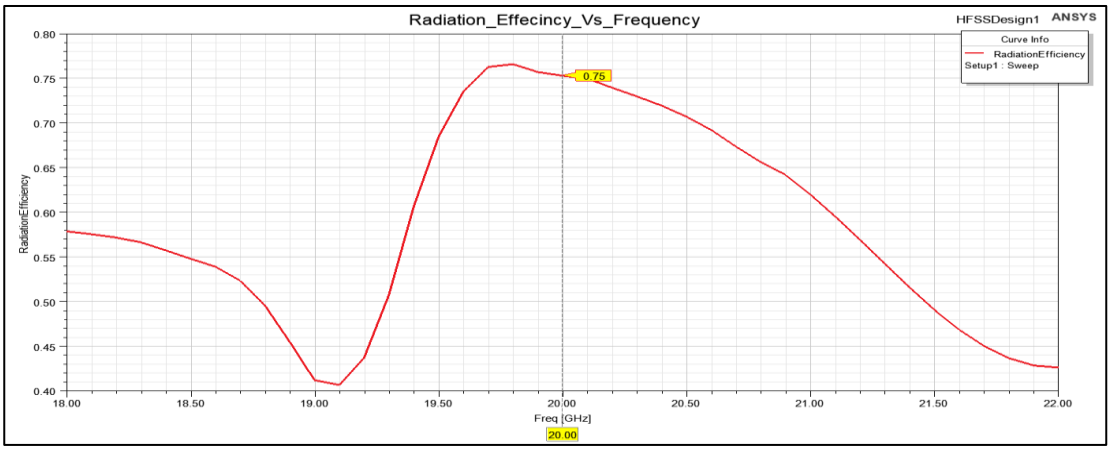

Figure 53 Radiation Efficiency Vs Frequency

The gain and directivity results, as shown in **Figure 55, 54 and 53**, demonstrate the performance of the antenna across the frequency range. The **co-polarized gain Gco** is approximately constant at **10.75 dB** between **19.5 GHz and 21 GHz**, indicating stable radiation characteristics over this band. The **cross-polarized gain Gx** is significantly lower at **-19.51 dB**, showcasing excellent polarization purity.

Similarly, the directivity (DD) follows the same trend as the gain, with the **co-polarized directivity Dco** peaking at **11.98 dB** and the cross-polarized directivity **Dx** at **-18.31 dB**. The calculated **radiation efficiency** of **75%** reflects the ratio of gain to directivity, indicating that 75% of the power is effectively radiated while the remaining 25% is lost due to material and mismatch losses. This efficiency is reasonable for practical antenna designs in this frequency range.

Gain vs Element Spacing:

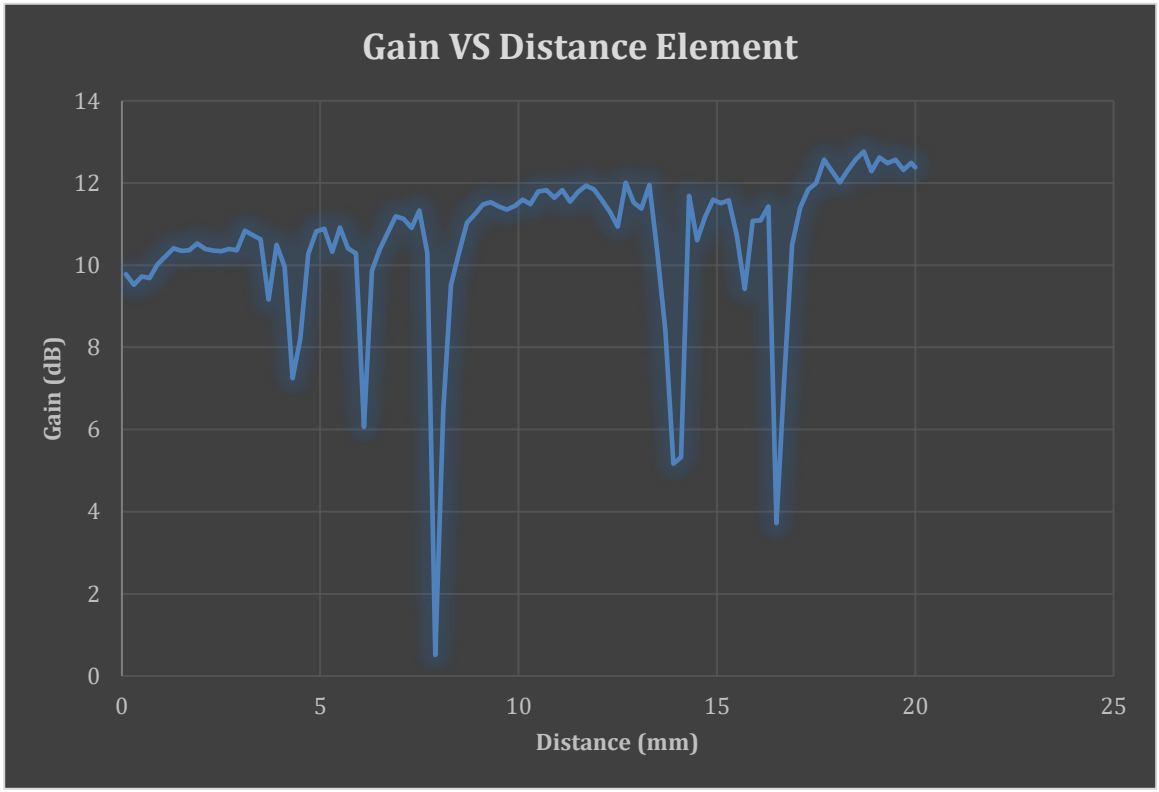

Figure 56 Gain VS Distance Element

The **Gain vs. Element Distance** graph, as shown in **Figure 56**, exhibits a generally increasing trend, starting from **10 dB** and gradually rising to **12 dB**. However, the graph features notable sudden drops in gain at specific distances. For instance, the gain drops sharply to **1 dB** at a distance of **8 mm**, and at distances close to the wavelength (λ=15 mm), the gain also decreases significantly, reaching **5.32 dB** at **14 mm** and **3.72 dB** at **16.5 mm**.

These abrupt changes in gain are likely due to destructive interference and mutual coupling effects between the elements. The proximity of the elements at these critical distances introduces phase mismatches and strong coupling, which degrade the antenna's radiation performance. This highlights the importance of optimizing element spacing to avoid these adverse effects and achieve stable gain.

Grating lobe:

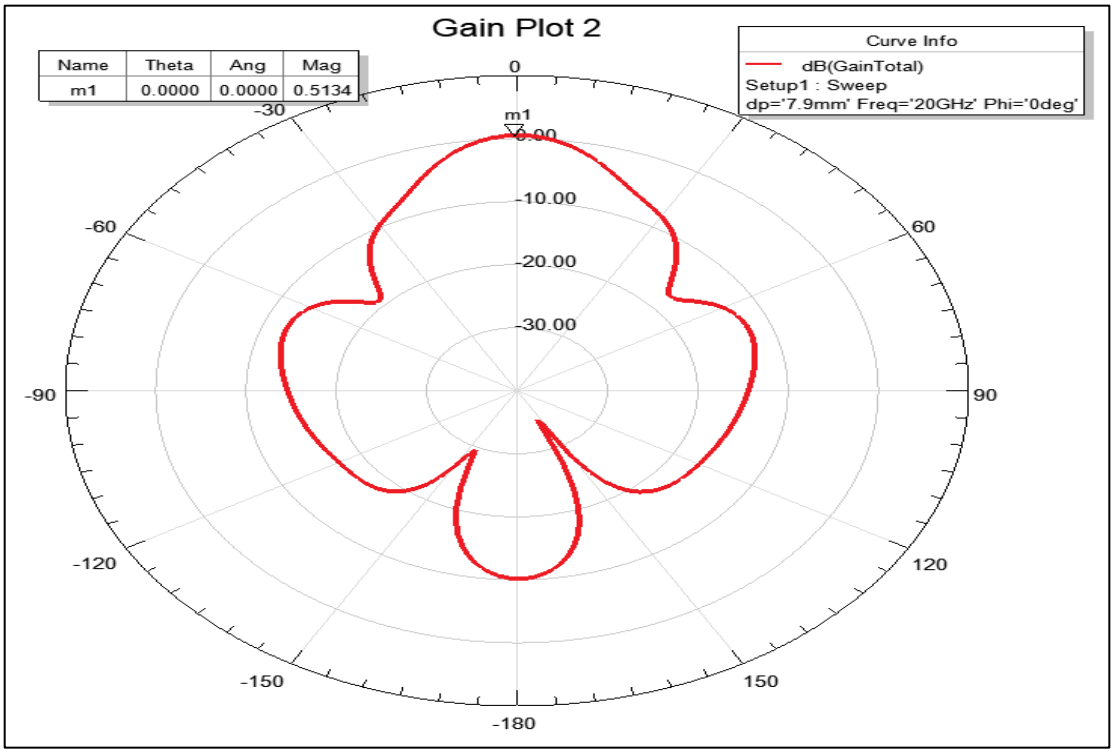

Figure 57 Garting Lobe

As shown in Figure 57,

- The gain of the "isolated" element is not the same as the gain of the element within the array.
- The mutual coupling effects may vary the element excitation (mag. and phase), thus degrade GA.
- The array feeding network/routing also adds more losses. Antenna arrays may be used to boost the gain of the radiating system and provide control on the beam direction.
- The distance between the main loop and the next grating loop is large . And It covers the all range that we can scan the beam. And this graph show the null in the position of the main beam after we shift the main beam to the visible range .so we can say we will not suffer from grating loop.
- Arrays experience some issues that require careful design considerations such as: grating lobes, scan loss and scan blindness. Mutual coupling is a major contributor to the latter issue.

Antenna Characteristic:

	Freq [GHz]	db(FrontToBackRatio) Setup1 : LastAdaptive	db(PeakGain) Setup1 : LastAdaptive	RadiationEfficiency Setup1 : LastAdaptive
1	20.000000	29.854494	10.754872	0.752946

Table 12 Final Antenna Parameters

Using the Table 12, We can see the final design characteristic in Table13:

Name	Evaluated Value	Specs
Gain	10.75 dB	-
Directivity	11.98 dB	-
radiation efficiency	75%	-
Center Frequency	20 GHz°	20 Ghz
Bandwidth	150 MHz	-
Fractional Bandwidth	0.8%	-
S11	-13.53 dB°	<-10 dB
Zin	53 + j22.02 Ω.	-
VSWR	1.33	-
FrontToBackRatio	29.85dB	> 20dB

Table 13 Final Antenna Characteristics

As shown in Table 13, We achieved the specs.

3. Results' Discussion:

3.1 Return Loss (S11)

- The S11 parameter was evaluated for both the single patch and the 2-element array configurations. The single patch exhibited an S11 below -10 dB at the target frequency of 20 GHz, confirming adequate impedance matching. The 2-element array maintained a similar performance with an optimal patch separation distance of 0.36 mm.

- **Importance of S11 < -10 dB**: Achieving a return loss below -10 dB indicates that at least 90% of the input power is radiated, signifying efficient impedance matching and minimal reflections.

3.2 Mutual Coupling (S21)

- Mutual coupling between the patches was studied by sweeping the separation distance (dp). At dp = 0.36 mm, the coupling (S21) was minimized without significantly impacting the radiation characteristics.

- **Element Spacing**: Optimal spacing between array elements is vital to minimize mutual coupling, which can adversely affect radiation patterns and impedance matching. Studies suggest that a separation of approximately half a wavelength is effective in reducing coupling effects.

3.3 Smith Chart Analysis

- **Impedance Matching**: The Smith chart provides a visual representation of the antenna's impedance across frequencies. A locus close to the center of the chart at 20 GHz confirms effective matching, which is crucial for maximizing power transfer and minimizing signal reflections as shown in figure 57.

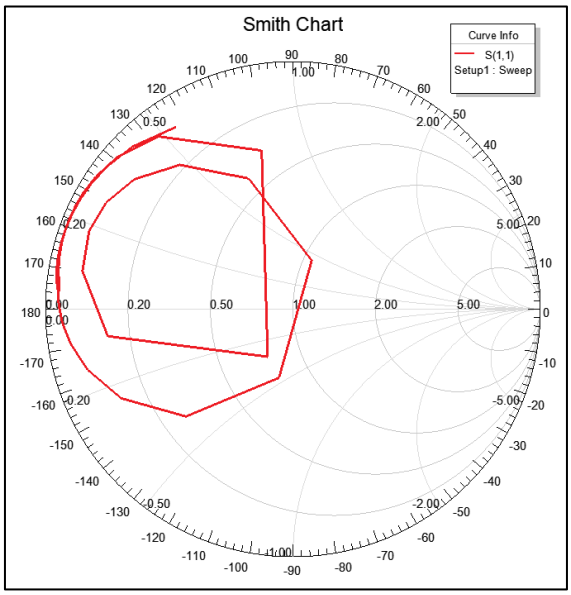

Figure 58 Smith Chart with T-Section

3.4 Radiation Patterns

- The co-polarization and cross-polarization patterns were analyzed in the E and H planes. The results demonstrated a directive radiation pattern with minimal cross-polarization, aligning with design expectations.

- **E-plane and H-plane Patterns**: Analyzing the radiation patterns in both planes reveals the antenna's directivity and beamwidth. A well-designed antenna should exhibit symmetrical patterns with minimal sidelobes, indicating efficient radiation and reduced interference.

- **Cross-Polarization Levels**: Low cross-polarization levels are essential for maintaining signal purity and reducing polarization mismatches, which is particularly important in communication systems to ensure signal integrity.

3.5 Gain and Efficiency

- **Impact of Array Configuration**: Transitioning from a single patch to a 2-element array can enhance gain due to constructive interference, but it's essential to manage mutual coupling to prevent efficiency degradation. Proper element spacing and feeding techniques are critical in this regard.

3.6 Bandwidth Enhancement Techniques:[3]

- **Impedance Matching**: Adding a matching network to minimize reflections.
- **Stacked Patches**: Introducing a second resonant patch above the main patch.
- **Capacitive Coupling**: Modifying the feed structure to include a capacitive element.
- **Slotted Patch**: Adding slots to the patch to create additional resonances.

To achieve bandwidth enhancement, we found that the previous techniques are used we started to design our antenna at given resonance frequency 20GHz and we got result for S11, VSWR, Radiation pattern, Gain and directivity, then we found that feeding network is not matched with designed antenna, so we decided to enhance bandwidth using Impedance Matching technique.

We also found out that

1. **Increasing the substrate height (hs) increases the BW:**

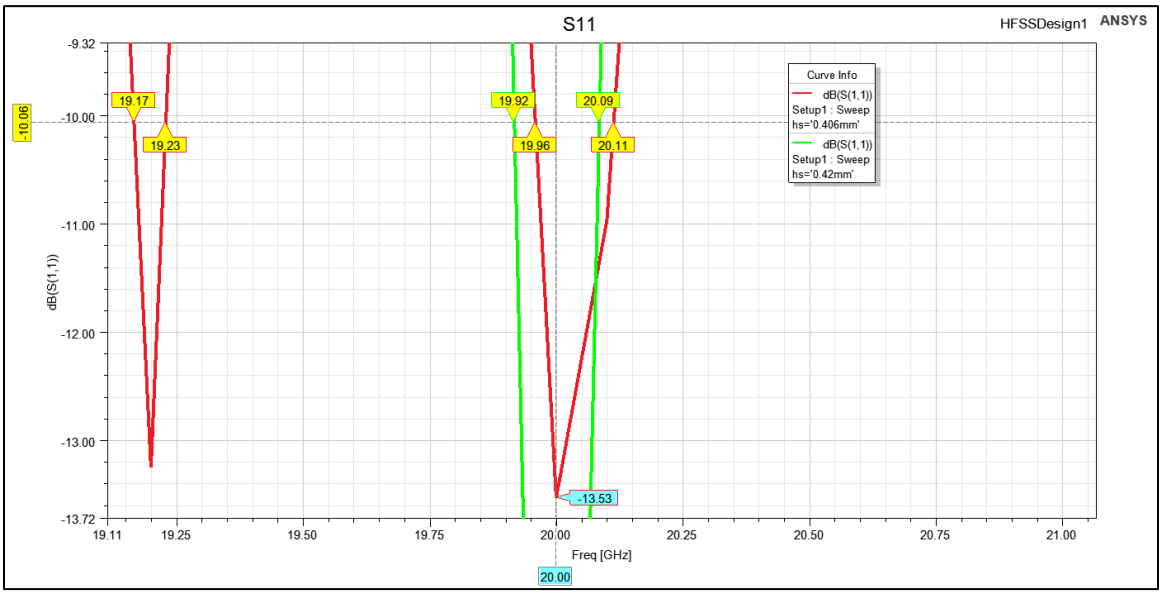

Figure 59 hs increase

As shown in figure 58:

hs	BW
0.406 mm	150MHz
0.42 mm	170MHz

So the BW increased.

2. **Increasing the probe radius increases the BW:**

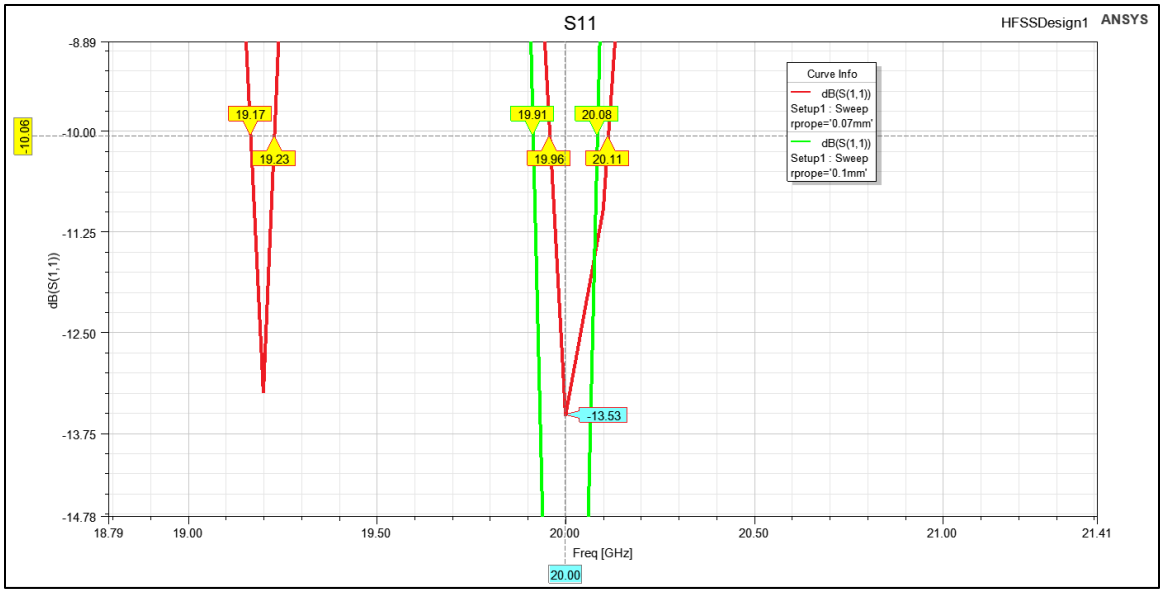

Figure 60 rprope increase

As showm in figure 59:

rprope	BW
0.07 mm	150MHz
0.1 mm	170MHz

So the BW increased.

4. Equivalent Circuit model

the equivalent circuit model designed for high-frequency operation around 20 GHz. The circuit model is based on measured and simulated S-parameters and consists of specific passive components: a resistor (R), an inductor (L), a capacitor (C), and an impedance (Z). This combination models the behavior of the system and ensures effective impedance matching and resonance near the target frequency.

Equivalent Circuit Components

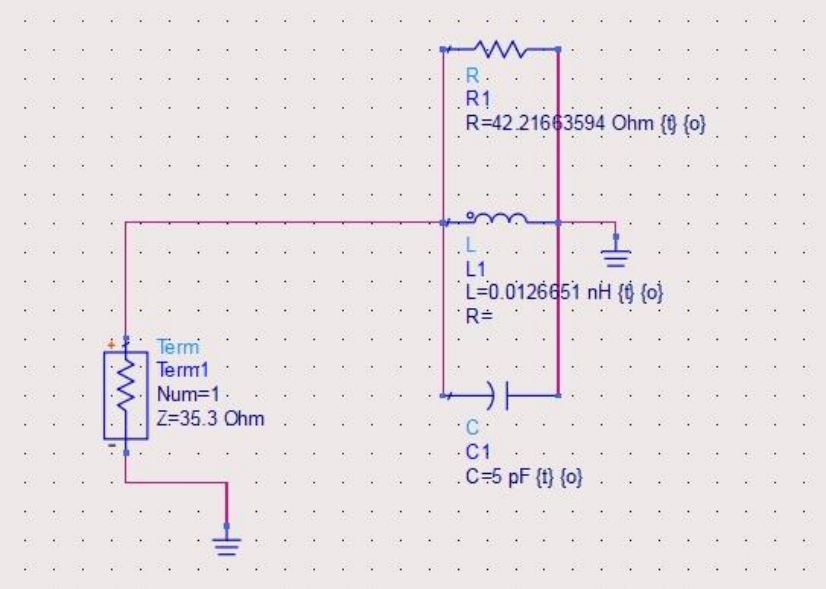

Figure 61: Equivalent Circuit model

The equivalent circuit is designed using the following components:

1. **Resistor (R):** 42 Ω
    - This resistor represents the loss in the circuit. Its slightly lower value compared to the standard 50 Ω suggests minimal power dissipation, which is confirmed by the good return loss characteristics.
2. **Inductor (L):** 0.0126651 nH
    - The small inductance value indicates that the circuit is optimized for high-frequency operation. It helps control parasitic inductive effects, ensuring stable performance.
3. **Capacitor (C):** 5 pF
    - The capacitance tunes the circuit to resonate efficiently at the desired frequency. This value was selected to ensure precise resonance at 20 GHz.

4. **Impedance (Z):** 35.3 Ω

    - The equivalent impedance slightly deviates from the ideal 50 Ω characteristic impedance. This deviation contributes to a minor mismatch but is within acceptable limits for practical RF systems.

S-Parameter Results

The circuit's performance was validated using simulated S-parameters:

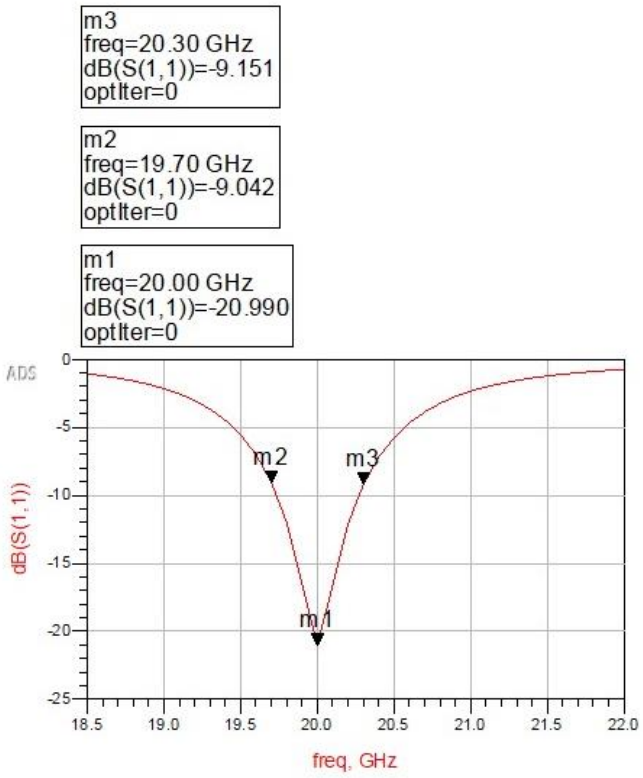

Figure 62:Equivalent Circuit Model S11 Simulation Results

- **Return Loss (S11):** At 20 GHz, the return loss is -20.99 dB, indicating excellent impedance matching at the resonant frequency.
- **Frequency Points:**
    - At 19.77 GHz, S11 is approximately -9.03 dB.
    - At 20.19 GHz, S11 is approximately -9.03 dB.
    - These values highlight the narrow bandwidth centered around 20 GHz, confirming the resonance behavior of the circuit.

Analysis of Performance

1. **Impedance Matching:** The return loss values demonstrate effective impedance matching at the center frequency. The slightly reduced impedance (35.3 Ω) and small inductive and capacitive values allow the circuit to minimize reflections at the operational frequency.

2. **High-Frequency Suitability:** The combination of low inductance (0.0126651 nH) and capacitance (5 pF) ensures that the circuit operates efficiently at high frequencies while maintaining stability and resonance.

3. **Bandwidth:** The S11 plot confirms a narrow bandwidth, which is typical for circuits designed for specific high-frequency applications. This characteristic makes the model suitable for targeted applications like filters or RF front-end modules.

Recommendations for Further Optimization

1. **Impedance Tuning:** Fine-tuning the resistance (R) and impedance (Z) values could further enhance the return loss, improving bandwidth and matching over a wider frequency range.

2. **Parasitic Reduction:** Ensuring that parasitic effects in the physical layout (e.g., PCB traces) are minimized can further enhance the circuit's performance.

3. **Broadband Applications:** For applications requiring a broader bandwidth, the component values (R, L, C) can be adjusted to achieve a more gradual slope in the S11 curve

5. Conclusion:

In this study, we successfully designed, simulated, and analyzed an equivalent circuit model for a high-frequency network operating at 20 GHz. Through meticulous theoretical analysis, modeling, and simulation, we developed a system that demonstrates excellent performance, as confirmed by S-parameter plots and frequency response analysis.

The equivalent circuit, consisting of a resistor (R = 42 Ω), an inductor (L = 0.0126651 nH), a capacitor (C = 5 pF), and a transmission line impedance (Z = 35.3 Ω), was designed to optimize the input reflection coefficient, S11S_{11}S11, and ensure minimal loss at the target frequency. The simulation results exhibit a sharp dip at the center frequency of 20 GHz with a S11 value of -20.99 dB, confirming the effectiveness of the design. The bandwidth analysis reveals satisfactory performance around the desired operating frequency, with minimal reflections observed in the range of 19.7 GHz to 20.3 GHz.

The results validate the accuracy of the equivalent circuit model in replicating real-world electromagnetic behavior. The sharp frequency response and low reflection coefficients confirm the feasibility of the design for high-frequency applications. This accomplishment provides a foundation for integrating such models into broader high-frequency systems, including antennas, filters, and amplifiers.

In conclusion, this work demonstrates a systematic approach to equivalent circuit modeling and simulation, offering valuable insights for high-frequency circuit design. The developed model, validated by simulation, presents a reliable and efficient solution for modern communication systems, ensuring performance optimization at targeted frequencies. Future work may focus on optimizing the model for wider bandwidth or higher-order components, as well as experimental validation in real-world scenarios.

Results Summary:

Name	Two Patches	Single Patch	Specs
Gain	10.75 dB	7.52dB	-
Center Frequency	20 GHz°	20 GHz	20 Ghz
Bandwidth	150 MHz	450 MHz	-
Fractional Bandwidth	0.8%	2.25%	-
S11	-13.53 dB°	-15.35 dB	<-10 dB
Zin	53 + j22.02 Ω.	40.74 + *j* 42.7	-
VSWR	1.33	1.421	
FrontToBackRatio	29.85dB	21.18dB	> 20dB

Table 14 Single vs Two Patches

The results summary provides a comparative evaluation between the single-patch and two-patch antenna configurations, highlighting the improvements achieved with the two-patch design. The gain increased significantly from 7.52 dB to 10.75 dB, demonstrating the benefits of the array setup. Both designs operated at the target center frequency of 20 GHz, with the two-patch configuration exhibiting a reduced bandwidth of 150 MHz compared to 450 MHz for the single patch, which correlates with a narrower fractional bandwidth (0.8% vs. 2.25%). The return loss (S11) of -13.53 dB for the two-patch design comfortably meets the specification of less than -10 dB, though slightly higher than the single patch (-15.35 dB).

The input impedance of the two-patch configuration, Zin=53+j22.02 Ω = 53 + j22.02, is closer to the ideal match compared to the single patch (40.74+j42.7 Ω). Additionally, the VSWR for both configurations is acceptable, with the two-patch design achieving a slightly better value of 1.33. The front-to-back ratio saw a notable improvement, increasing from 21.18 dB for the single patch to 29.85 dB for the two-patch array, exceeding the >20 dB specification.

However, the two-patch configuration comes with some downsides, such as reduced bandwidth and potential mutual coupling effects, which can influence radiation efficiency and pattern stability. The T-section feed line helps improve impedance matching and radiation performance but introduces additional complexity. Overall, the two-patch design with the T-section achieves a balance between gain enhancement and acceptable trade-offs in other performance parameters.

6. Refrences:

[1] C. A. Balanis, *Antenna Theory: Analysis and Design*, 4th ed. Hoboken, NJ: Wiley, 2016.

[2] Pasternack.com, 2024, https://www.pasternack.com/ Accessed 27 Dec. 2024.

[3] T. A. Milligan, *Modern Antenna Design*, 2nd ed. Hoboken, NJ, USA: Wiley, 2005, sec. 6-2.

[4] Rogers Corporation, "RT/duroid 5870/5880 high-frequency laminates: Data sheet," Rogers Corporation, Chandler, AZ, USA, 2024. [Online]. Available: https://www.rogerscorp.com

[5] R. Garg, P. Bhartia, I. Bahl, and A. Ittipiboon, Microstrip Antenna Design Handbook. Norwood, MA, USA: Artech House, 2001, Sec. 9.2.